NASA CONTRACTOR REPORT

NASA CR-2378

NASA CR-2378

NON-ENGINE AERODYNAMIC NOISE INVESTIGATION OF A LARGE AIRCRAFT

by John S. Gibson

Prepared by
LOCKHEED-GEORGIA COMPANY
Marietta, Ga. 30063
for Langley Research Center

NATIONAL AERONAUTICS AND SPACE ADMINISTRATION • WASHINGTON, D. C. • OCTOBER 1974

1. Report No.	2. Government Accession No.	3. Recipient's Catalog No.
NASA CR-2378		

4. Title and Subtitle	5. Report Date
NON-ENGINE AERODYNAMIC NOISE INVESTIGATION OF A LARGE AIRCRAFT	October 1974
	6. Performing Organization Code

7. Author(s)	8. Performing Organization Report No.
John S. Gibson	
	10. Work Unit No.

9. Performing Organization Name and Address	11. Contract or Grant No.
Lockheed Aircraft Corporation Lockheed-Georgia Company 86 South Cobb Drive Marietta, GA 30063	NAS1-12443
	13. Type of Report and Period Covered
12. Sponsoring Agency Name and Address	Contractor Report
National Aeronautics & Space Administration Washington, DC 20546	14. Sponsoring Agency Code

15. Supplementary Notes

This is a final report.

16. Abstract

A series of flyover noise measurements have been accomplished utilizing a large jet transport aircraft with engine power reduced to flight idle. It was determined that the aerodynamic (non-engine) noise levels did occur in the general range that had been predicted by using small aircraft (up to 17,690 kg gross weight) prediction techniques. The test procedures used are presented along with discussions of the effects of aerodynamic configuration on the radiated noise, identification of noise sources, and predicted aerodynamic noise as compared with measurements.

17. Key Words (Suggested by Author(s))	18. Distribution Statement
Aerodynamic noise Non-engine noise	Unclassified - Unlimited STAR Category 02

19. Security Classif. (of this report)	20. Security Classif. (of this page)	21. No. of Pages	22. Price*
Unclassified	Unclassified	55	$3.75

*For sale by the National Technical Information Service, Springfield, Virginia 22151

CONTENTS

NON-ENGINE AERODYNAMIC NOISE INVESTIGATION OF A LARGE AIRCRAFT

By

John S. Gibson

Lockheed-Georgia Company

SUMMARY

Previous noise measurements and prediction procedures for non-engine aerodynamic noise were based on glider and small aircraft data (590 kg to 17,690 kg gross weight). The purpose of this program was primarily to determine if the aerodynamic noise levels of a very large aircraft did occur in the general range predicted by small-aircraft prediction techniques. To verify large aircraft predictions, a series of flyover noise measurements were made under a C-5 Galaxy aircraft. The engines were cut back to flight idle, so that engine noise would have a minimum effect and could be separated from the non-engine aerodynamic noise. This type of experimental procedure was successful, and effective measures of aerodynamic noise were made from very low frequencies, through the expected peak aerodynamic noise range, and on up to the engine turbo-machinery noise range.

Effects of aerodynamic configuration were evaluated, particularly those relating to wing-flap and landing gear extension. Time histories of flyover noise showed complex variations of noise with time. Three specific noise source areas were identified: (1) airflow over and from the wings, (2) airflow around the landing gear and wheel wells, and (3) trailing vortex wake. The first two are the most significant. Other possible secondary sources and subdivisions of the main sources were investigated, but no firm identifications could be made.

Peak aero noise frequencies and levels were close to those predicted. Wing-related noise had a narrower bandwidth than expected, resulting in less high-frequency noise and lower perceived noise levels than expected for an aerodynamically "clean" aircraft. The spectrum shape for normal, aerodynamically "dirty" landing configuration aircraft was essentially as predicted, and perceived noise as well as overall noise levels were close to those predicted. Therefore, it is concluded that the primary objective of the experimental program was met. In addition, more insight was gained into the basic noise mechanisms involved.

INTRODUCTION

The subject of non-engine aerodynamic noise (sometimes called "self-noise" or "airframe noise") was concerned until recently with noise radiation from small, military surveillance aircraft. Here the problem was to reduce noise so that the aural detection distance from an observer to the aircraft was at a minimum. To determine the contribution of non-engine aerodynamic noise (hereafter usually referred to as aero noise) to the aural detection problem, noise measurements and analyses were made of the flyovers of gliders and unpowered small aircraft (eg., Ref. 1).

During the recent (1971 - 72) NASA sponsored Advanced Technology Transport Study Program, a complete systems analysis of advanced subsonic transport design was undertaken. This effort looked into noise problems in detail. Quiet aircraft and engine designs were investigated to get aircraft total noise levels as low as 20 EPNdB below current FAR 36 criteria levels. When it appeared that the conventional noise sources of a transport aircraft could be reduced on this order, it was necessary to investigate any additional possible noise "floors" or "barriers" that might prevent reaching the desired low noise levels. The generation and radiation of aero noise appeared to be a potential problem. The technology resulting from the small-aircraft programs was then applied to the large advanced subsonic aircraft under study, and surprisingly high noise levels were predicted (Ref. 2). A typical predicted spectrum is shown in Figure 1. Subjective noise predictions for a typical case (gross takeoff weight 272,000 kg) for the three FAR 36 locations were: takeoff flyover 92 EPNdB, takeoff sideline 86 EPNdB, and landing approach flyover 97 EPNdB, where the current criteria limit for all three cases is 108 EPNdB.

The predicted level is relatively high on takeoff flyover, but is about 16 EPNdB below the criteria. At the sideline point, the predicted level is 22 EPNdB below the criteria. Unless the engine noise levels and criteria are reduced by 15 to 20 EPNdB on takeoff and sideline, aero noise would not be expected to have a great effect. However, on landing, the predicted 97 EPNdB is only 11 EPNdB under the criteria. Thus, the large reductions in noise of new, quieter engines might not be effective in the landing case, if the aero noise predictions were realistic.

In order to determine if the aero noise levels of a very large aircraft did occur in the general range predicted, and to find out more about the possible mechanisms involved (Figure 2), it was felt that aero noise measurements were needed on a very large aircraft. The appropriate measurements were made under low-altitude flyovers of a Lockheed C-5 "Galaxy" transport. This report describes the experimental procedures and results of the flyover noise measurement program.

EXPERIMENTAL RESULTS AND ANALYSIS

Experimental Procedures

To explore the extent and nature of the aero noise problem, an investigation of C-5 "Galaxy" flyover noise, inflight with low engine power, was undertaken. Figure 3 shows, for reference, the overall dimensions and shape of the aircraft. The basic idea was to concentrate on the low-frequency range, where non-engine aerodynamic noise was expected to peak, and not to use the mid- to high-frequency range noise data known to be the range of engine fan tones. Also, low-frequency engine jet noise was expected to be 10 to 20 dB below non-engine aero noise. Thus, an acoustic "window" existed in the frequency range of expected maximum aero noise levels, bounded on the bottom by engine jet noise and in the high-frequency range by the fan fundamental. Any noise appearing in the "window" is assumed to be aero noise. A description of the "window" and a typical example of flyover data compared with static data are given in Figure 4. Little change would be expected in the strong fan tones with forward speed, and little was observed. Some reduction in jet noise could be expected due to the relative velocity effect on jet noise. Therefore, the bottom boundary of the "window" could actually be lower than that shown in Figure 4. (Further discussion of this subject appears in a later section.)

Details of the experimental program are presented below.

Microphone Location - The microphone station was located at the west end of the main runway at Dobbins AFB, Georgia, in a flat, grassy overrun area, 140 meters from the pavement on the extended runway centerline. The general location is given in Figure 5.

Instrumentation and Equipment - B&K Type 4132 (2.54 cm) microphone and windscreen, 1.5 meters above ground; B&K Type 2204 sound level meter; Nagra A.M. tape recorder for noise data acquisition. Data reduction was accomplished on a B&K Model 3329 one-third-octave-band analyzer, and an EMR 6040 computer with a fast Fourier transform program for narrow-band work. Altitude, gross weight, airspeed, were obtained from the aircraft. The pressure altimeter was calibrated with the ground station on each run. Weather data were obtained from the Dobbins AFB weather office.

Procedure - The time history of each aircraft flyover was recorded on tape. The aircraft approached from the west using flight idle engine power until well past the measuring station, then full power was applied for go-around. Target altitude over the measuring station was 100 meters. Actual altitudes ranged from 36 to 146 meters.

Date and Weather Conditions - 1st Test Series, January 18, 1973.

Temperature	15.6°C
Relative Humidity	73%
Wind	2.3 m/s, N.W.
Barometer	763 mm of Hg.

- 2nd Test Series, March 12, 1973

Temperature	17.0°C
Relative Humidity	69%
Wind	3.6 m/s, N.W.
Barometer	753 mm of Hg.

Test Runs and Aircraft Configurations - Details regarding test runs and aircraft configurations are given in Table 1. In addition, dimensions which were constant are: wing span, 68.0 meters; average wing chord, 8.6 meters; and average wing thickness, 0.86 meters. Lockheed flight test airplane, Serial Number 0003, was used for all noise measurements.

Aerodynamic Configuration Effects

One of the objectives of the experimental program was to determine the differences between the spectrum shapes for an aerodynamically "dirty" aircraft (with landing gear, flaps, and leading-edge slats extended) and an aerodynamically "clean" aircraft (all devices retracted). Photographs of the various configurations are shown in Figures 6, 7, and 8. The first, Figure 6, is the takeoff configuration, shown for information only, since no data were taken at this condition. The landing configuration is shown in Figure 7 and Figure 8 shows the "clean" configuration with all landing devices retracted.

Figures 9 through 13 show third-octave spectra (peak levels) for all test runs in the first series. Figure 9 is the spectrum resulting from a "clean" configuration flyover. This spectrum, below the fan fundamental, has a peaked broadband shape that corresponds to predicted fluctuating lift force/vortex shedding noise from the wing. The measured peak frequency in the broadband area corresponds rather closely to the predicted Strouhal frequency for wing-flow noise (discussed in a later section). These apparent semi-discrete frequencies occur in a fairly high Reynolds number range (4.0×10^6 to 6.0×10^6, based on wing thickness), even though one recent laboratory investigation could find no discrete frequency emission from a small airfoil at Reynolds numbers above 2.4×10^6 (Ref. 3).

Figures 14 through 18 are narrow-band plots for all first-series test runs. (These, and other narrow-band plots in this study, were made from a 1.5-second segment of time just after the peak flyover noise levels occurred. The effective analyzer bandwidth was 1.0 Hz for all narrow band plots.) Figure 14 is a narrow-band plot showing that, not only does a wing fundamental appear, but also an array of additional discrete frequencies appear throughout the spectrum. All these cases show a second hardmonic, which in one case was as high as the fundamental (Figure 18). It is suspected that angle of attack, which was not constant during the tests, could have caused considerable variations in fundamental-to-harmonic relationships. The characteristic frequency of fluctuating drag forces also is double the frequency of the larger fluctuating lift forces. It does not appear that fluctuating drag-force noise could be as significant as fluctuating lift-force

noise, since drag forces are so much smaller and predominantly radiate in the wing plane, unless some sort of interaction occurs between the two sources.

Figure 11 is an inflight third-octave-band plot of a typical "dirty" configuration test run. The spectrum below the fan fundamental is full of peaks, with rather high levels below the wing fundamental. Therefore, the combined effects of lowering landing gear and extending flaps and slats have greatly broadened the spectrum. The wing fundamental and harmonic can still be seen in all the "dirty" configuration runs (Figures 10 through 13). In narrow-band form (Figures 15 through 18), these same spectra indicate that most of the increases in noise level are also due to discrete or semi-discrete frequency emissions, rather than to broadband emissions such as might be expected in boundary-layer noise.

Since the "dirty" configuration spectra appear to be somewhat insensitive to flap and slat extension on the wing, it is felt that most of the noise increases are associated with the landing gear and wheel well, with only a slight trend toward increasing noise with increasing flap extension. This is not entirely a conclusive result, since noise related to the landing gear/wheel well could be masking or interacting with flap effects.

A second series of three test runs was made to improve the isolation of flap effects. Here, only flap extension was varied as a test parameter. However, due to the nature of the test procedure, velocity and angle of attack were not constant for the three test runs. These results also did not conclusively show the flap extension effects. Compared with the first series, the relative amplitude of the wing fundamental and harmonic reversed in one case (Run B-1, "Clean"). This is shown, along with the two other spectra, in Figure 19. When the second series of runs are normalized to the same velocity and altitude, the intermediate flap setting gave the highest level and full flap the lowest, further confusing the issue. One point which could have affected the results (in addition to angle-of-attack effects) of the second test series was the fact that the aircraft altitudes were very low, from 36 meters to 50 meters; this probably put the microphone in the acoustic near field of the wing noise source. It should be recalled that the wing source itself is almost 68 meters across. Therefore, it is felt that the second series of test results should not be compared with the first series on an absolute basis.

The following discussion is a possible explanation of the absence in either series of the strong flap effects which were expected. The aircraft has six individual flaps on each wing, each separated by a flap track fairing, as shown in Figure 7. The result is that, with increasing flap extension, the wing trailing edge is becoming irregular with flap segments of different sizes and fairings protruding aft. At high flap angles, there is also an air gap between a portion of each adjacent flap, as shown in Figures 6 and 7. The overall effect is apparently an irregular wing trailing edge that breaks up or decorrelates any large-scale fluctuating lift and turbulence formations, thereby reducing noise. This is the same concept that was thought to be one of the features of the "quiet" flight of owls which was propounded in 1934 by Graham (Ref. 4).

The effects noted in this test are not expected to be the same on all aircraft. Most aircraft have one or two long flaps, from which strong, correlated turbulence phenomena could be expected. Therefore, on most current aircraft, greater increases in noise level with increasing flap extension may be expected than was experienced here.

Time-History Analysis

Time histories in each one-third octave band, up to and including the fan fundamental, are given in Figure 20 for a 40% flap, retracted landing gear case (Run B-2). The zero time point corresponds to the time of peak wing noise (100 Hz one-third-octave band); minus time is time before peak, and plus time is time after the peak. Peak wing noise time corresponds approximately to the time the wing inboard trailing edge is directly over the measuring station. The correlation between peak wing noise time and aircraft location was done visually and is good to about ± 1/8 second. This test run had the cleanest signal for the entire time history. It was also the run with the lowest aircraft altitude and the highest signal levels. It should further be recalled that the measuring station in this case is in the acoustic near field.

Examining the time histories, starting at the low-frequency end, it is evident that there is a double-peak trend, most pronounced at 63 Hz. As the frequency goes higher, a new double peak trend is seen at 100 Hz (peak wing noise), and a triple peak at 125 Hz. At 200 Hz, a new triple peak is evident, close together in time with the central peak predominant. Going on to much higher frequencies, it is evident that the fan noise fundamental peaks at 630 Hz, just after zero time. This corresponds to known static fan noise directivity, which is not expected to be affected significantly by the relatively low aircraft forward speed. The numerous small peaks and valleys provide much in the way of questions which cannot yet be answered. Some peaks may be due to fluctuating drag forces on certain aerodynamic surfaces. These would be expected to peak at other points than directly overhead. They may also be the result of harmonics of the primary fluctuating forces, or could be partially the effect of ground to microphone interference.

It is also interesting to note that peak wing noise (100 Hz) and peak fan noise (630 Hz) have similar rise-and-fall characteristics as a function of time. These rise-and-fall times are similar to those of the total noise of other unsuppressed turbofan engine aircraft at the same altitude with low engine power (e.g., see Ref. 5).

Noise-Source Study

In a previous section, the basic noise effects of the two primary noise sources, wings and landing gear/wheel well, were discussed. It was also shown that wing fundamentals generally fell in the 100Hz to 125 Hz range, and a prominent harmonic at twice those frequencies. When the landing configuration was measured, numerous peaks above and below the wing fundamental appeared. It would be informative to know what causes

these additional noise peaks (refer to Figure 2), as well as some of the minor peaks in the "clean" configuration spectra. Table 2 contains predicted near-field noise generation frequencies for several likely noise sources, other than the wing, over a range of aircraft velocities. Very little is known about how these other aerodynamic phenomena propagate to the ground, and no attempt is made here to calculate such propagation. Typical noise-source frequencies that do match up with ground-noise measurement may be radiating and warrant further investigation. The following discussion is thus based on limited technology and limited experimental data and is intended primarily to stimulate further, more exhaustive investigations. All of the discussion revolves around the data presented in Table 2.

Wheel Wells - The nose and main wheel well cavities typically would produce strong discrete frequencies with some broadband noise. This results from aero/acoustic resonances that occur in cavities with flow over them, and the turbulent flow interaction within and coming from the cavity. At relatively low speeds, such as occurs for landing aircraft, a modified Strouhal relationship, based on cavity length, works well for predicting peak frequencies for large wheel-well type cavities (Ref. 6). Table 2 shows that most predicted frequencies in the test velocity range fall below 25 Hz, and the measured data obtained are valid only down to about 20 Hz. However, it does appear that many low-frequency peaks in the very low-frequency range (see Figures 15 through 18) could be cavity resonances, and perhaps the peak that occurs just above 20 Hz in several spectra is the primary resonance of the nose-wheel-well cavity.

Landing Gear - The landing gear wheels themselves create broadband noise due to random turbulence created by the flow over them. The landing gear struts probably have some vortex shedding which would produce discrete frequencies and broadband noise. Calculated frequencies, based on a Strouhal relationship as a function of strut diameter (Ref. 6), cover the range from just over 30 Hz to 81 Hz. Since there are so many measured peaks in this range, it is difficult to identify any particular one as being definitely from this source, but it is a good possibility.

Aerodynamic Shaped Surfaces - The aerodynamic surfaces, other than the wing, are the pylons, the vertical stabilizer, and the horizontal stabilizer. Noise should be generated by vortex shedding and turbulence in a similar manner to that of the wing (predictions based on Ref. 2). Table 2 shows that the frequency range from 33 Hz to 261 Hz could have contributions from these sources. Again, it is difficult to identify any particular measured peaks, but the possibility of correlation does exist both above and below the wing fundamental.

Airflow over Airframe - This source, usually referred to as "boundary layer noise," does produce rather high local surface fluctuating pressure levels, but it is generally thought to radiate poorly. It is readily heard inside the fuselage. The noise generated is very broadband, and the peak frequencies on the fuselage, for example, cover a wide range, 150 Hz to 1200 Hz (unpublished Lockheed data). As much of this noise is masked by engine noise, no particular effects can be identified on the ground. On a large aircraft, however, the surface areas involved are large, and it is conceivable that some of the

measured broadband background noise does come from this source. It will probably not be significant until some of the other noise-producing sources are reduced.

Fuselage Wake - Fuselages with upswept aft ends, like that of the Galaxy, can produce a wake of shed vortices and turbulence in a manner similar to a plain cylinder (Ref. 7). This type of fuselage acts like a cylinder at an angle to the flow. The resulting noise spectrum could contain discrete frequencies and broadband noise. Predicted fundamental frequencies are in the inaudible range, as indicated in Table 2. While this phenomenon can be felt as vibration inside an aircraft under certain conditions, it is not thought to be a significant far-field noise source. The turbulence field produced does eventually become a part of the trailing vortex wake of the aircraft and is measurable as described in a previous section.

Nacelle Airflow - With the engines at very low power, there is a possibility of some broadband noise being generated from air spillage from the inlet and consequent flow around the engine nacelle. The level and peak frequencies of such noise are unknown.

Structural Vibration - The possibility of structural vibration as a noise source was found in one instance. Referring to Figure 17, noise peaks can be seen at 25 and 35 Hz. Figure 21 is a plot of main wheel-well door vibration (see Figures 6 and 7 for door detail), with similar double-peak response frequencies in the 30 Hz to 40 Hz range. While the inflight vibration data were not taken in the identical flight conditions as the noise test, this does point up the strong possibility that structural vibration can cause some noise radiation to the ground.

Noise Predictions and Actuals

The noise-prediction procedure used to calculate the Galaxy aero noise levels is described in the Appendix. This procedure, based on small aircraft technology (590 kg to 17,690 kg gross weight), is for "clean" configuration aircraft. In previous estimates of noise levels for large aircraft in the "dirty" landing configuration, 5 dB and 5 PNdB were added to the "clean" predictions of OASPL and PNL, respectively.

It should be pointed out that an updating of the prediction procedure, including the use of data from this program, is the subject of a concurrent separate contracted effort (Contract NAS 1-12440). The purpose of this experimental program was primarily to determine, by limited full-scale testing, if the aero noise levels of a very large aircraft did, in fact, occur in the general range predicted. It was not the intent to obtain large amounts of repeatable data under very controlled conditions to develop a refined noise-prediction procedure. However, discussion of how the early prediction procedure compares with actuals does warrant consideration and is the subject of this section. The following discussion revolves around Table 3.

First consider Run A-1 which was for the "clean" configuration. The predicted OASPL for the spectrum with engine noise removed, as estimated in Figure 9, is within

0.6 dB of the predicted level. The PNL is some 5.4 PNdB lower than that predicted. The main reason for the large difference in PNL is the fact that the measured "clean" spectrum is much steeper than predicted and, therefore, contains less high-frequency noise which is very PNL sensitive.

Now consider Run A-5 which is a full "dirty" configuration flyover. Here the OASPL is 6.8 dB higher than predicted, the spectrum is broadband and similar to that predicted, and the PNL is 7.9 PNdB higher than predicted. Based on this run alone for "dirty" configuration effects, the estimated 5 PNdB increase added to a "clean" prediction was nearly correct. However, the total difference between "clean" and "dirty" configurations, based on the difference between the two runs, is 13.3 PNdB. This is somewhat higher than the 9 PNdB reported after a preliminary evaluation of some of the early data (Ref. 8). The large relative difference in PNL (as opposed to a difference of only 7.4 dB in OASPL) is primarily the result of the difference in shape of the "clean" measured spectrum which was not considered in the prediction process. These trends are similar to the results obtained on a 747 aircraft, where a "clean" to "dirty" effect of 10 to 12 PNdB was found (Ref. 9).

The main contributor to "dirty" configuration noise appears to be the landing gear area. As evidenced for Runs A-2, A-3, A-4, all of which had landing gear down and 0% to 40% flaps, the actual noise levels in terms of OASPL are from 2.6 dB to 3.7 dB higher than predicted, and the PNL's are 2.1 PNdB to 3.3 PNdB higher than predicted. Therefore, even at 0% flaps, but with the landing gear extended, noise levels are considerably higher, and the spectrum shape broader than for the "clean" run A-1 (see Figures 9 through 13 for spectrum shapes).

The net result is that there does appear to be a 3 to 4 dB OASPL and 3 to 4 PNdB PNL increase effect for 100% flap extension as compared to 0% or 40% flaps, all with gear extension. If the total full "dirty" configuration effect is on the order of 13 PNdB, and 3 to 4 PNdB is due to the flaps, then the remaining 9 to 10 PNdB are due to the landing gear. The relatively small flap effect may be explained as being related to flap design, as stated in a previous section. The large landing gear effect may be due to the larger than usual "soft field" landing gear and wheel well of the Galaxy as compared with most other "hard field" transports.

The second series of runs, as stated previously, gave somewhat unexpected and inconsistent results in spectrum shape and level. It should be remembered that these runs were all taken at very low altitudes and are assumed to be in the acoustic near-field. Since the noise level prediction procedure is strictly far-field, predicted versus actual results for these cases are assumed to be meaningless and are not considered further. However, for completeness, 2nd test series data are included in Table 3.

In terms of predicted peak wing noise frequency, near-field or far-field conditions should have essentially no effect. The results of both series of tests do show predicted to actual agreement to within 20%, some much better, except for one case at 23%. Since some actuals are higher and some lower than predicted, the frequency prediction procedure is assumed to be essentially correct within the simplified ground rules from which it was derived.

Other Observed Effects

Jet Noise Level in Flight - A partial substantiation of the reduction of jet noise due to the forward speed of the aircraft was determined. Figure 22 presents a plot of the aero noise portion of a "clean" configuration run (Test Run A-1, from Figure 9), along with a plot of the static jet-noise spectrum (from Figure 4). The low-frequency skirt of the "wing" aero-noise spectrum should drop off as indicated by the dashed downward extension, rather than leveling off at 75 dB. The jet velocity from the primary and fan nozzles are both approximately only 88 meters/second at flight idle, which falls in the range of aircraft forward velocities encountered in this test program. Therefore, the relative jet velocity compared with the atmosphere is essentially zero, and jet noise should drop appreciably. If it is assumed that jet noise does drop, it must be concluded that the reason for the lack of a much greater "relative velocity" reduction is the fact that, at very low jet velocities, "excess jet noise" or other "tailpipe" noise sources are holding the level up, even though "pure jet mixing" noise may be much lower.

Trailing Vortex Wake Noise - After one of the low flybys (Run A-5), and when the aircraft was about 1600 meters away, the trailing vortex wake was clearly audible. Figures 23 and 24 show the measured third-octave and narrow-band spectra of this noise phenomenon. To a ground observer, vortex wake noise is characterized by a general "rushing" sound similar to low-velocity jet noise, with the addition of some faint "crackling" or "popping" sounds. The "cracking" sound is believed to be associated with the beginnings of vortex breakup. The peak frequency is rather low, and this noise source is not expected to be a problem, except that it might keep low-frequency noise levels up sufficiently to lengthen the time between the 10 dB down points on a flyover noise time history. This could possibly increase the level of an Effective Perceived Noise Level calculation.

CONCLUSIONS

The main objective of this test program was to determine if the aero noise levels of very large aircraft did occur in the general range predicted. Since the peak frequencies and levels did appear essentially as predicted, it is concluded that this primary test objective was met.

Three noise source areas were identified: (1) wing noise, (2) landing gear/wheel well noise, and (3) trailing vortex noise. The first two components are the most significant.

Of the major source areas on the Galaxy, the landing gear/wheel well area produced the largest increase when going from "clean" to "dirty" configurations. The flaps had a lesser effect, probably due to the rather unusual aerodynamic design. The total effect of going from a "clean" to a "dirty" configuration on the Galaxy is 7.4 dB in OASPL and 13.3 PNdB in PNL.

Wing-related noise has a narrower bandwidth than that predicted based on the small aircraft data. This is the reason for the larger differences in predicted versus actual PNL's as compared to OASPL's for the "clean" configuration.

Noise data measured at approximately a wing span or greater behaved as if in the far field, whereas data measured at less distance was inconsistent, and is probably in the near field.

Some evidence was found to give a partial confirmation of the drop in low-frequency jet noise due to aircraft forward speed.

TABLE 1

TEST RUN AND CONFIGURATION DETAILS

TEST SERIES	RUN	FLAP EXTENSION*	LANDING GEAR	AIRSPEED METERS/SECOND	ALTITUDE METERS	WEIGHT KILOGRAMS	C_L	ANGLE OF ATTACK RADIANS
1st (1-18-73)	A-1	Up (0 rad)	Up	102	91	275,335	0.74	+ 0.087
	A-2	Up (0 rad)	Down	103	91	282,593	0.76	+ 0.097
	A-3	40% (0.279 rad)	Down	90	146	279,418	0.99	+ 0.065
	A-4	40% (0.279 rad)	Down	86	91	278,057	1.03	+ 0.068
	A-5	100% (0.698 rad)	Down	72	55	276,696	1.48	+ 0.092
2nd (3-12-73)	B-1	Up (0 rad)	Up	93	50	244,944	0.80	+ 0.099
	B-2	40% (0.279 rad)	Up	93	36	243,130	0.80	+ 0.033
	B-3	100%(0.698 rad)	Up	85	44	241,315	0.93	0.0

* Leading-edge slats are extended to a single fixed position when flaps are at any position except completely up. 100% flap is the landing configuration; 40% is approach configuration.

TABLE 2

PREDICTED FUNDAMENTAL OR PEAK FREQUENCIES FOR OTHER THAN WING NOISE SOURCES

NOISE SOURCE	FREQUENCIES (Hz) (airspeed - m/s) 50	75	100	TYPICAL CHARACTERISTICS	ESTIMATED PROBABLE SIGNIFICANCE
Nose Wheel Well	17	26	34	Fundamental, Harmonics, Broadband	Very High
Main Wheel Well	8	12	16	Fundamental, Harmonics, Broadband	High
Nose Landing Gear	41	61	81	Fundamental, Harmonics, Broadband	High
Main Landing Gear	32	49	65	Fundamental, Harmonics, Broadband	Very High
Engine Pylons	82	123	164	Fundamental, Harmonics, Broadband	Medium
Horizontal Stabilizer	131	196	261	Fundamental, Harmonics, Broadband	Medium
Vertical Stabilizer	56	33	111	Fundamental, Harmonics, Broadband	Medium
Boundary Layer - Fwd.	600	900	1200	Peaked, Very Broadband	Low
Boundary Layer - Mid	300	450	600	Peaked, Very Broadband	Low
Boundary Layer - Aft	150	225	300	Peaked, Very Broadband	Low
Fuselage Wake	4	6	8	Peaked, Very Broadband	Very Low
Nacelle Airflow		Unknown		Estimated to be Broadband	Low
Wheel Well Door Vibration	35	35	35	Fundamental, Harmonics	High

TABLE 3

NOISE PREDICTIONS VS. ACTUALS

TEST SERIES	RUN	CONFIGURATION	OVERALL SOUND PRESSURE LEVEL dB		PEAK WING FREQUENCY Hz		PERCEIVED NOISE LEVEL PNdB	
			PRED.	ACTUAL	PRED.	ACTUAL	PRED.	ACTUAL
1st (1-18-73)	A-1	Clean	101.1	100.5	130.4	110.0	104.7	99.3
	A-2	Partially Dirty	101.2	104.2	131.7	120.0	104.9	108.0
	A-3	Partially Dirty	93.5	96.1	114.6	120.0	96.4	98.5
	A-4	Partially Dirty	96.8	100.5	110.6	100.0	99.5	103.8
	A-5	Full Dirty	96.5	103.3	92.2	120.0	98.2	106.1
2nd (3-12-73)	B-1	Clean	103.8	106.8	118.5	120.0	106.7	107.9
	B-2	Partially Dirty	106.7	112.1	118.5	100.0	109.9	111.8
	B-3	Partially Dirty	102.6	101.3	108.6	120.0	105.4	101.3

NOTE: (1) See Table 1 for complete details of configuration, conditions, etc., for each run.

(2) These predictions are all for "clean" aerodynamics. No additions have been made to account for "dirty" aerodynamics, since the object is to see what differences are created by "dirty"configuration effects.

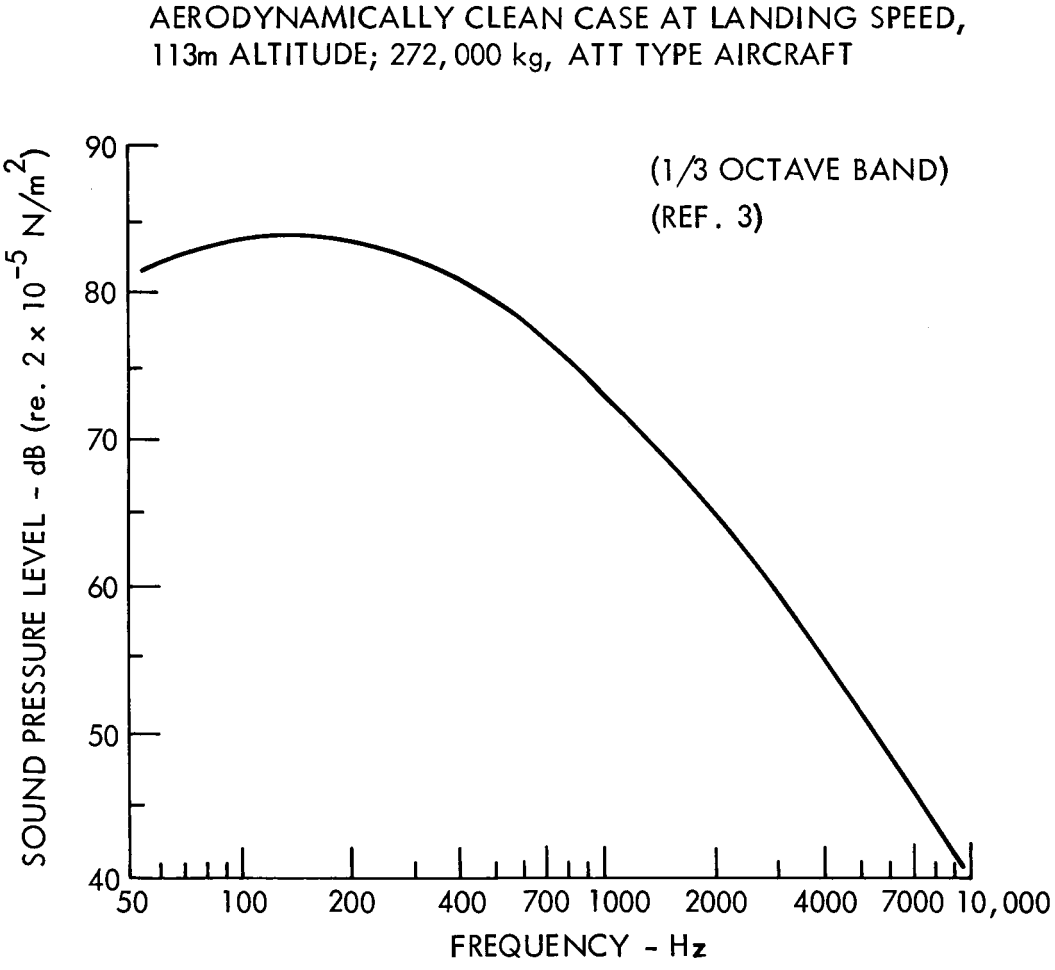

FIGURE 1 PREDICTED AERODYNAMIC NOISE SPECTRUM

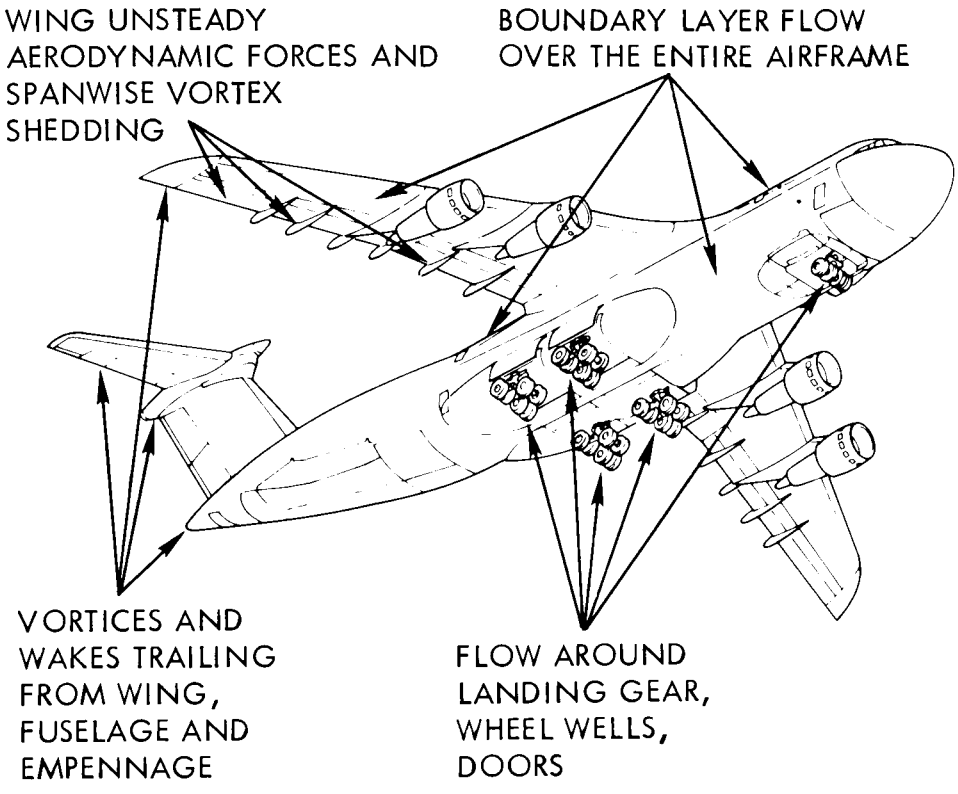

FIGURE 2 AERODYNAMIC NOISE SOURCES

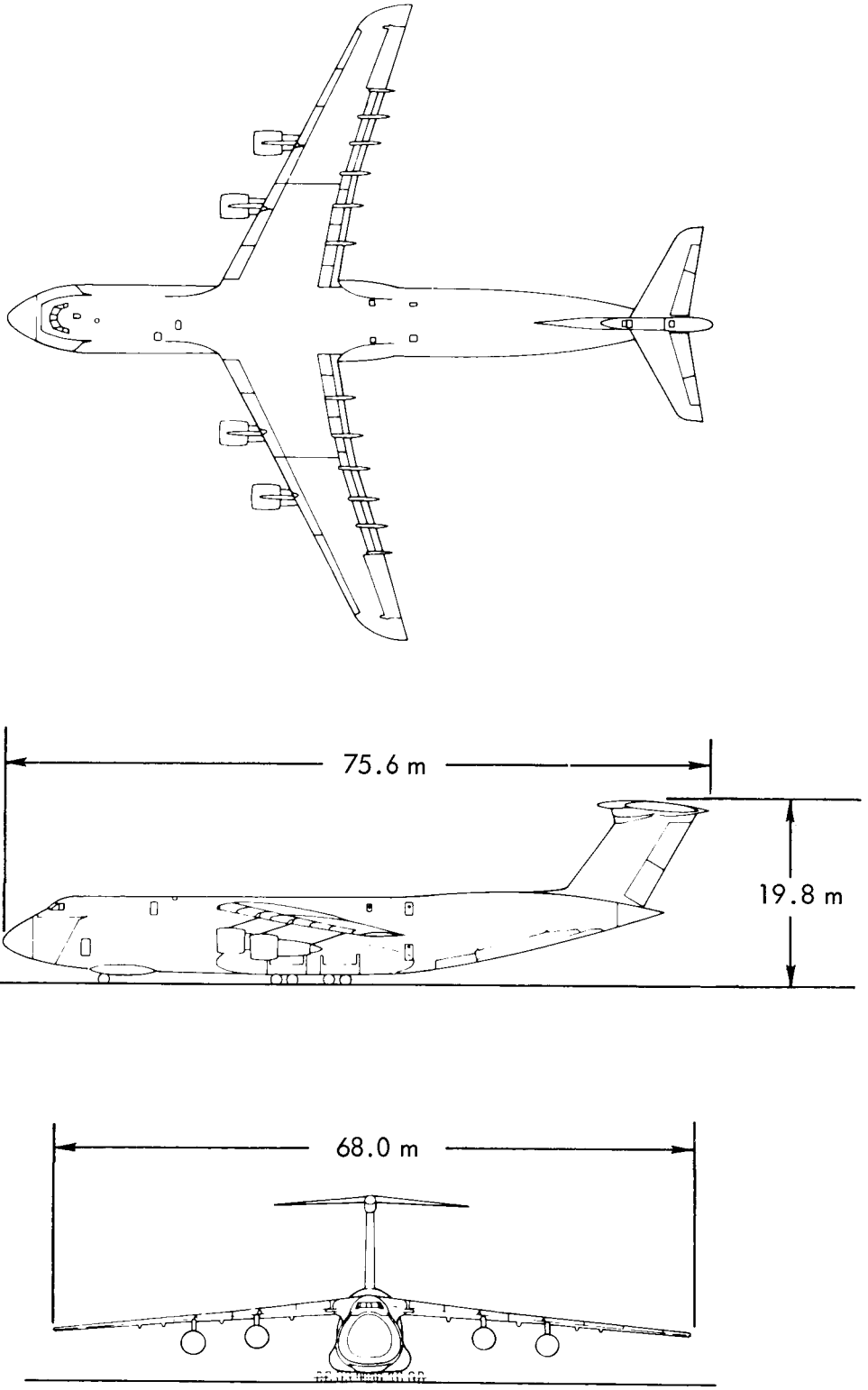

MAX TAKEOFF GROSS WT - 346,777 kg

FIGURE 3 GALAXY GENERAL ARRANGEMENT

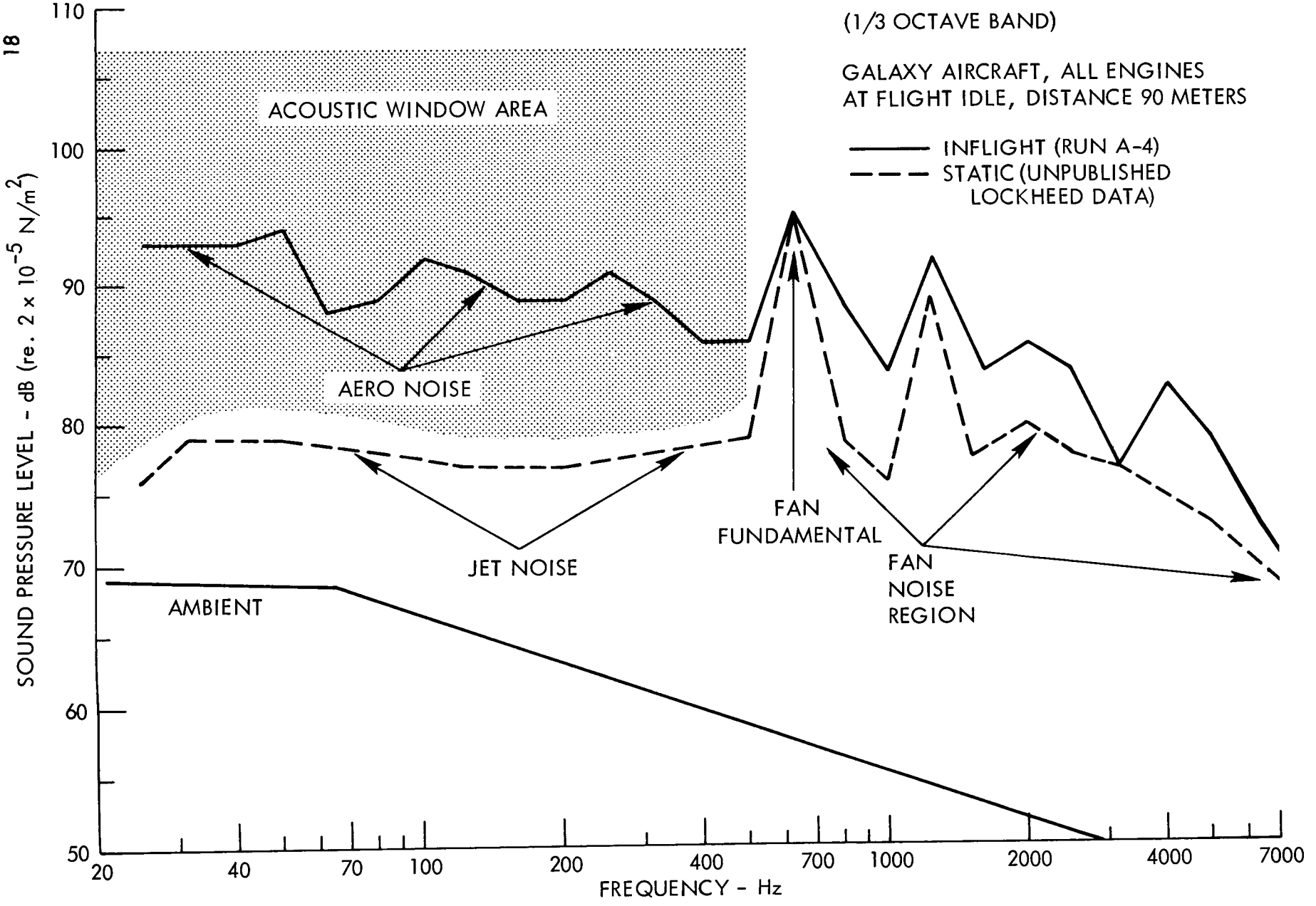

FIGURE 4 AERODYNAMIC NOISE DATA INTERPRETATION METHODOLOGY

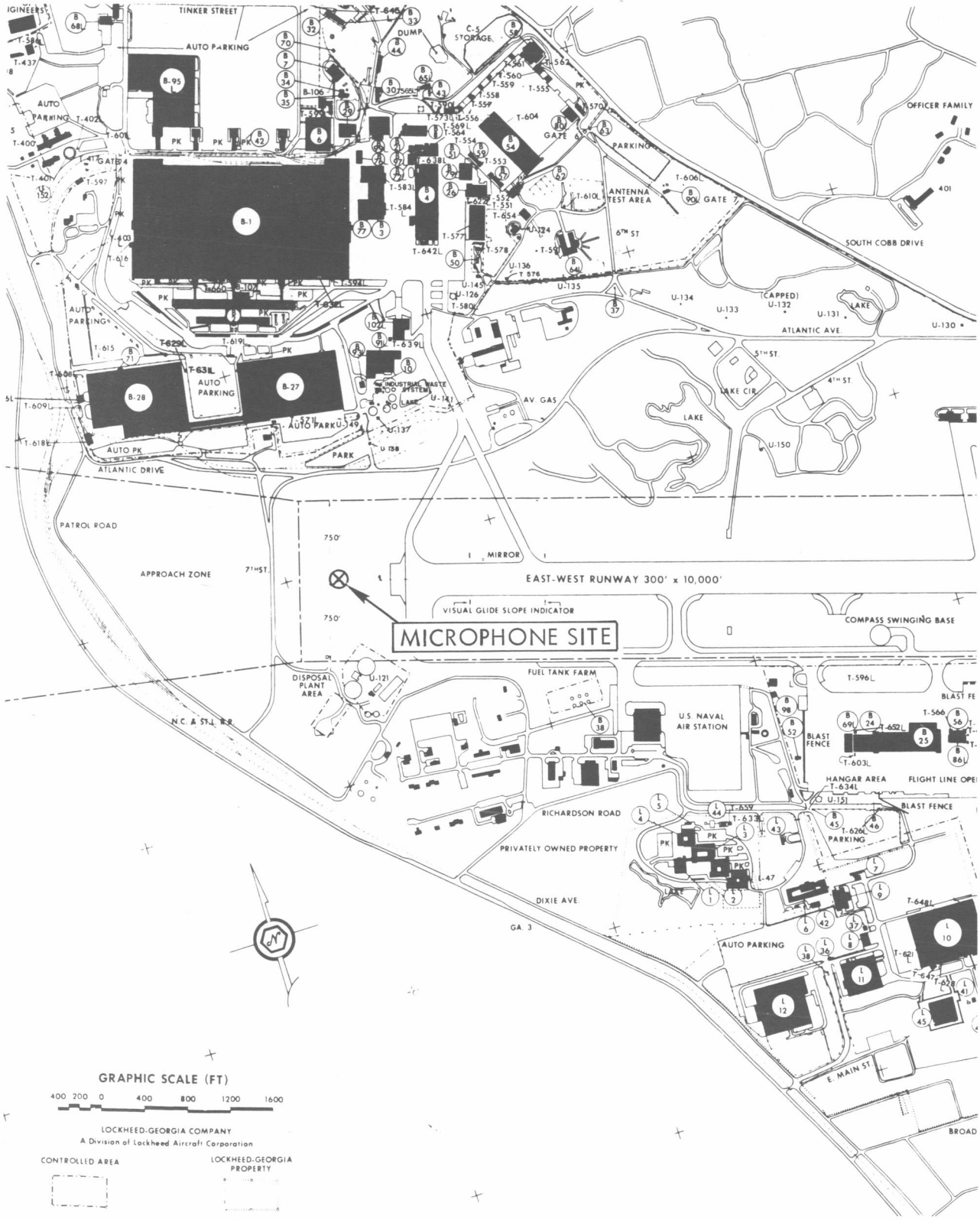

FIGURE 5 NOISE MEASUREMENT LOCATION

FIGURE 6 GALAXY IN THE TAKEOFF CONFIGURATION

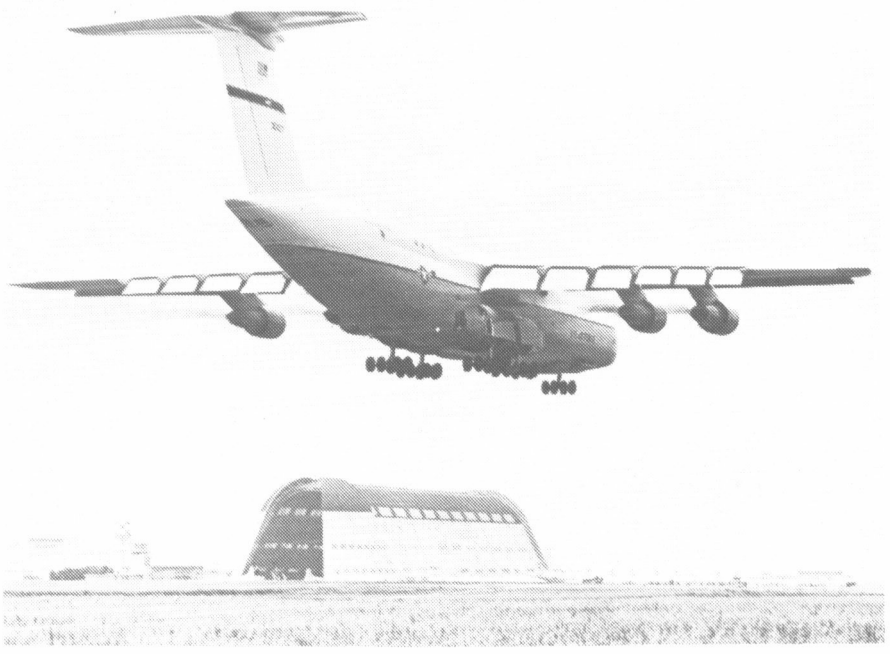

FIGURE 7 GALAXY IN THE LANDING CONFIGURATION

FIGURE 8 GALAXY IN THE "CLEAN" CONFIGURATION

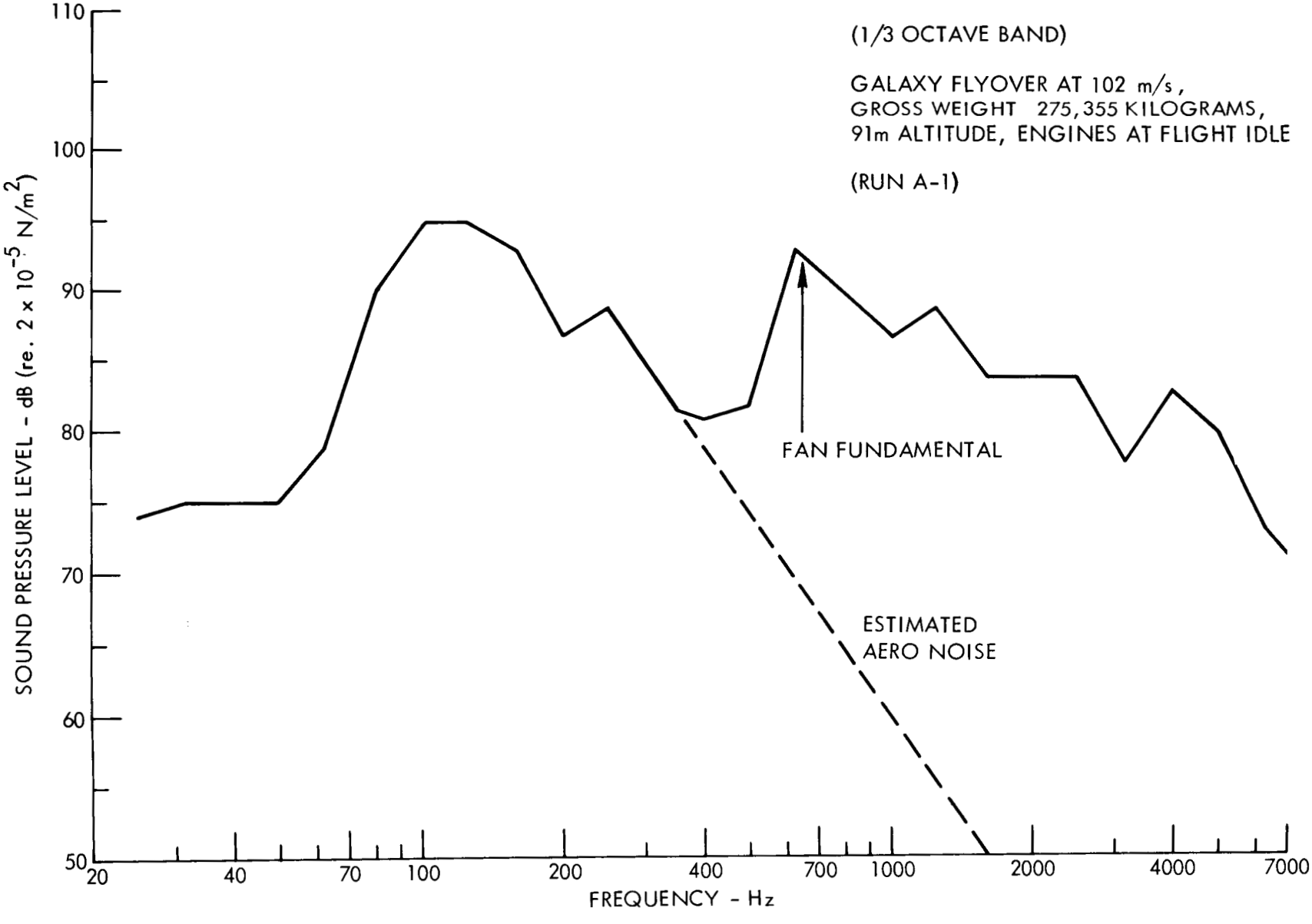

FIGURE 9 NOISE SPECTRUM FOR "CLEAN" CONFIGURATION

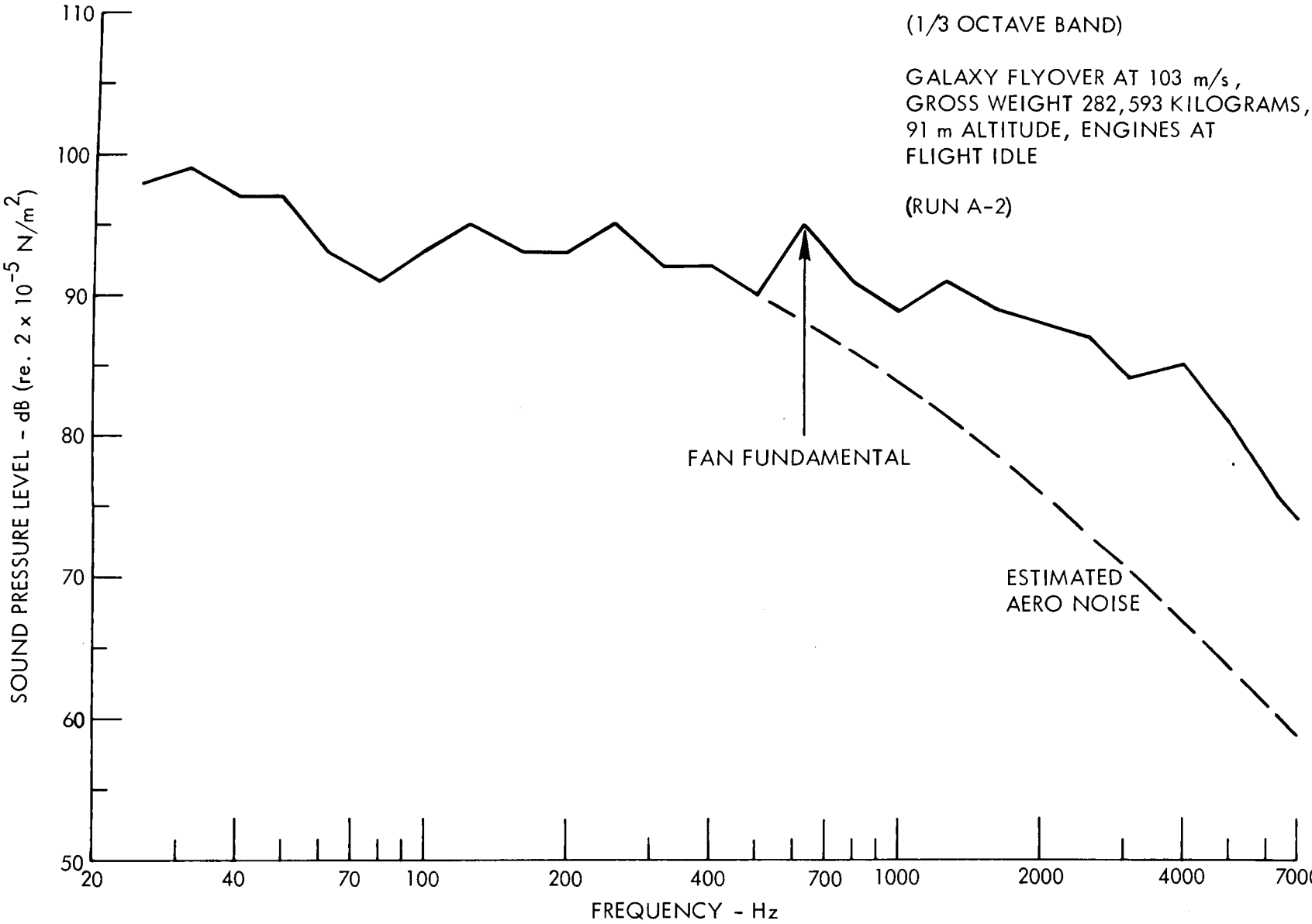

FIGURE 10 NOISE SPECTRUM FOR "CLEAN" WING, LANDING GEAR EXTENDED

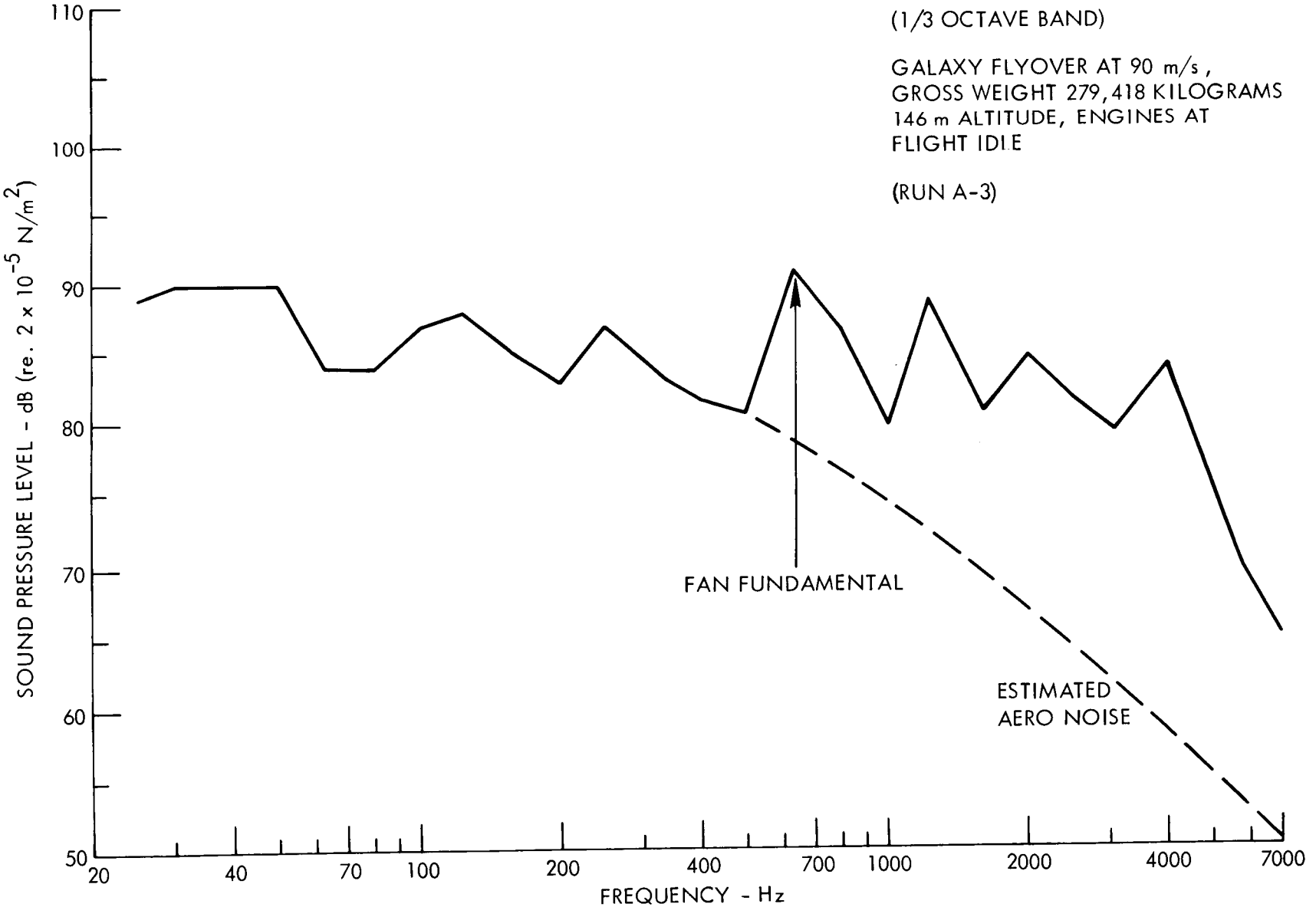

FIGURE 11 NOISE SPECTRUM FOR 40% FLAPS, LANDING GEAR EXTENDED

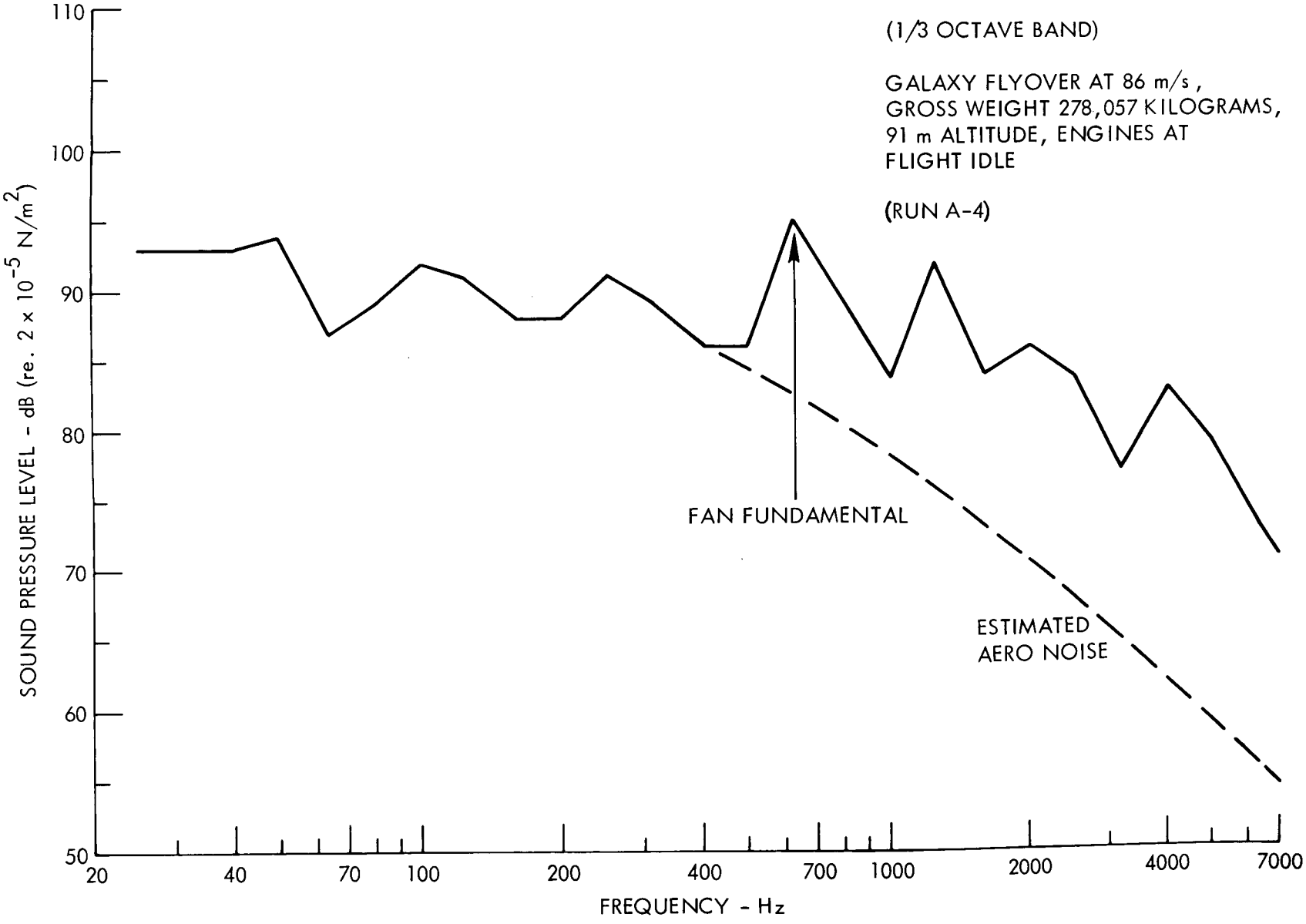

FIGURE 12 NOISE SPECTRUM FOR 40% FLAPS, LANDING GEAR EXTENDED

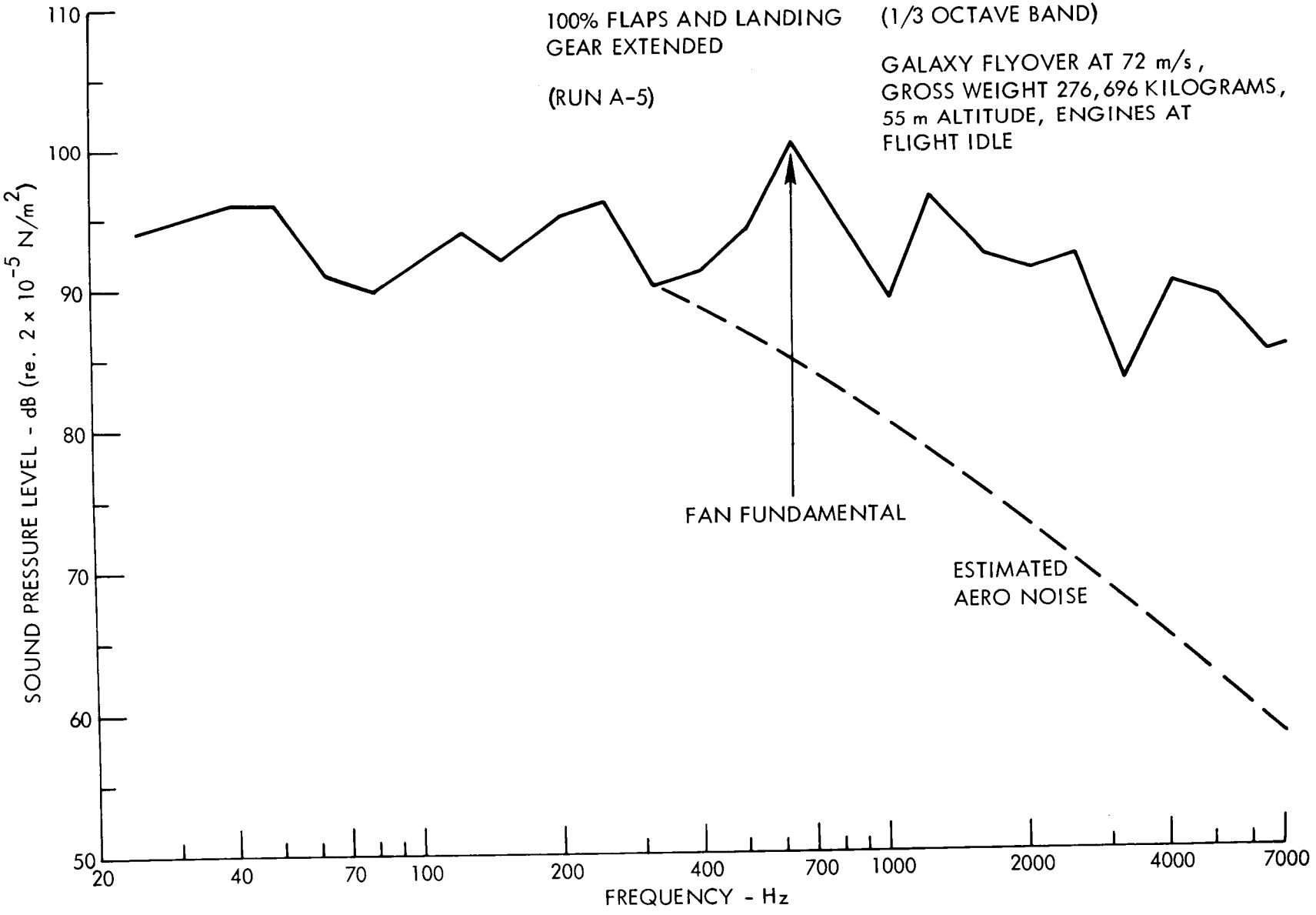

FIGURE 13 NOISE SPECTRUM FOR "DIRTY" CONFIGURATION

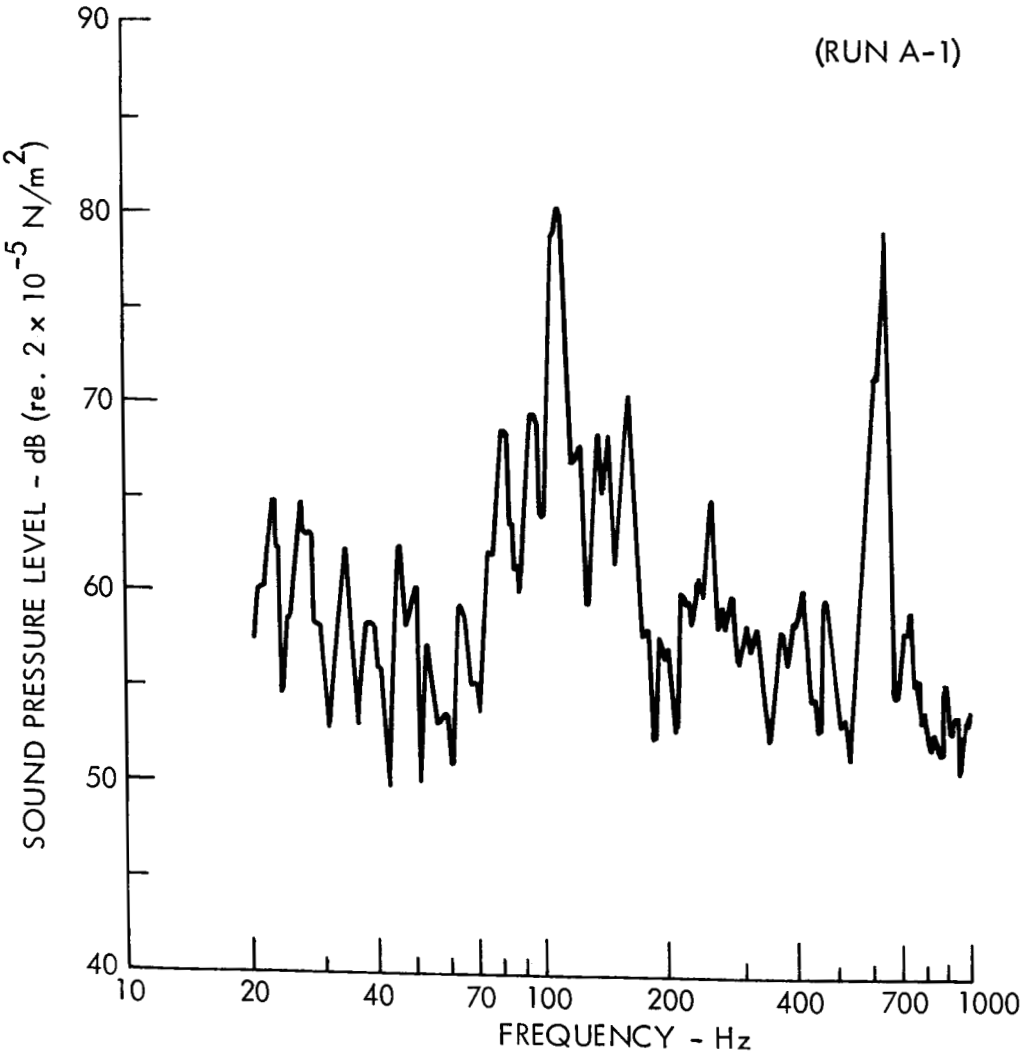

FIGURE 14 NARROW BAND SPECTRUM - "CLEAN" CONFIGURATION

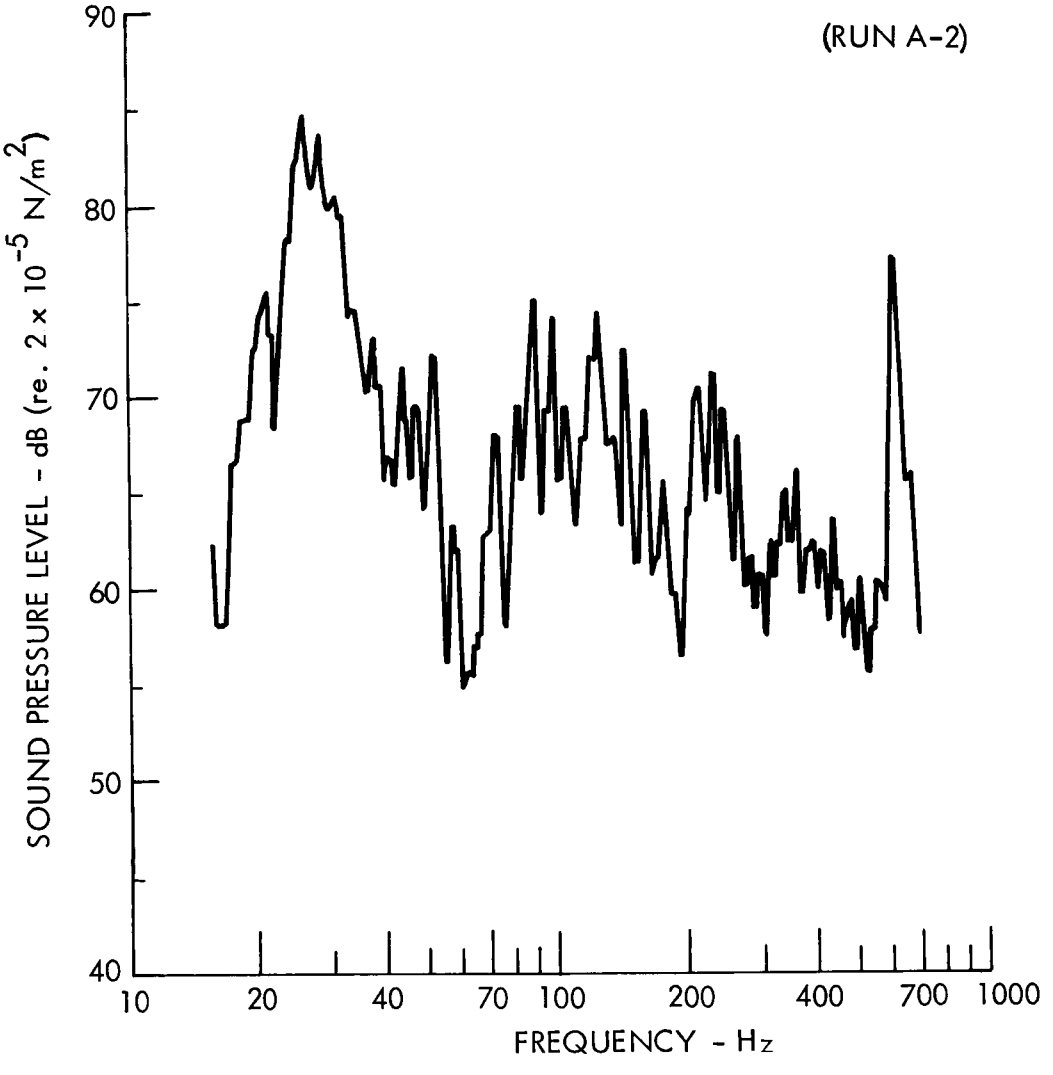

FIGURE 15 NARROW BAND SPECTRUM - CLEAN WING, LANDING GEAR EXTENDED

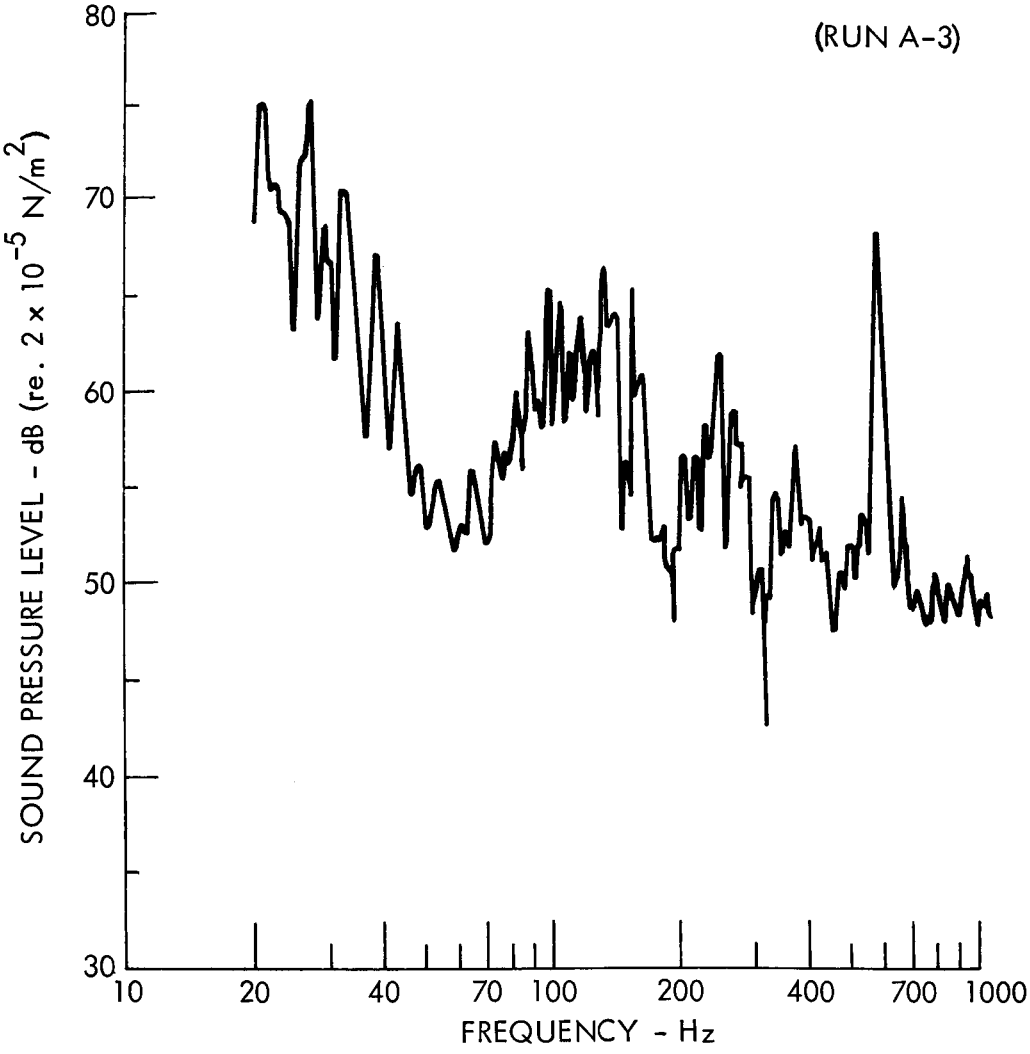

FIGURE 16 NARROW BAND SPECTRUM - 40% FLAPS, LANDING GEAR EXTENDED

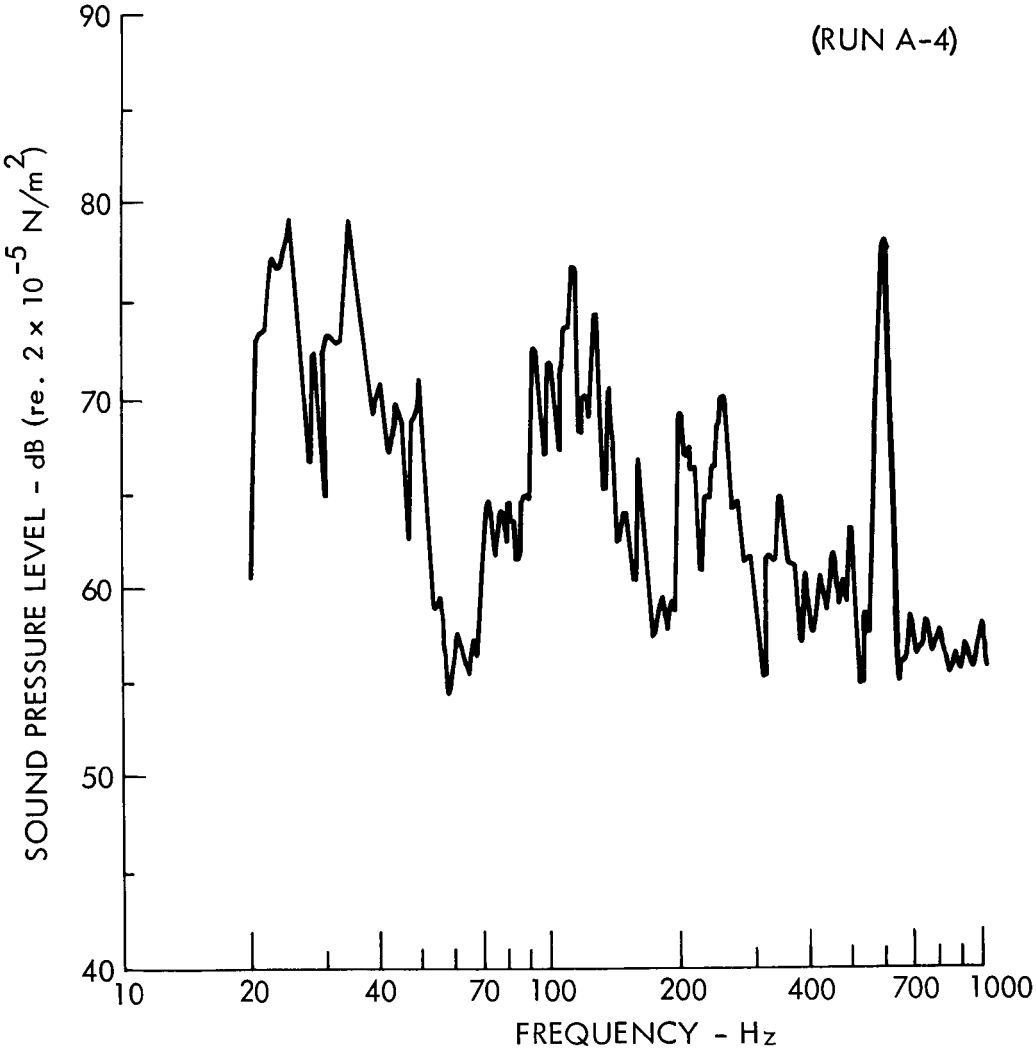

FIGURE 17 NARROW BAND SPECTRUM - 40% FLAPS, LANDING GEAR EXTENDED

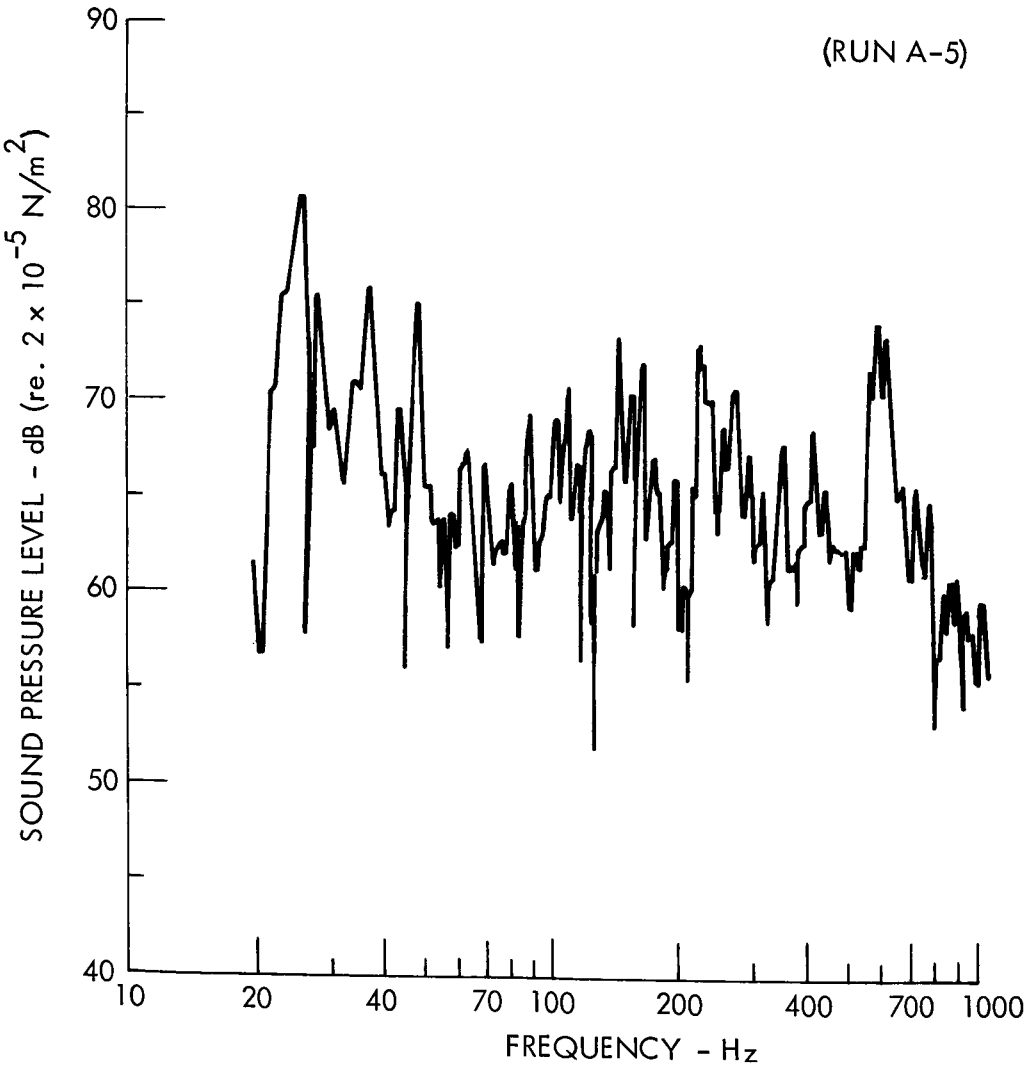

FIGURE 18 NARROW BAND SPECTRUM - "DIRTY" CONFIGURATION

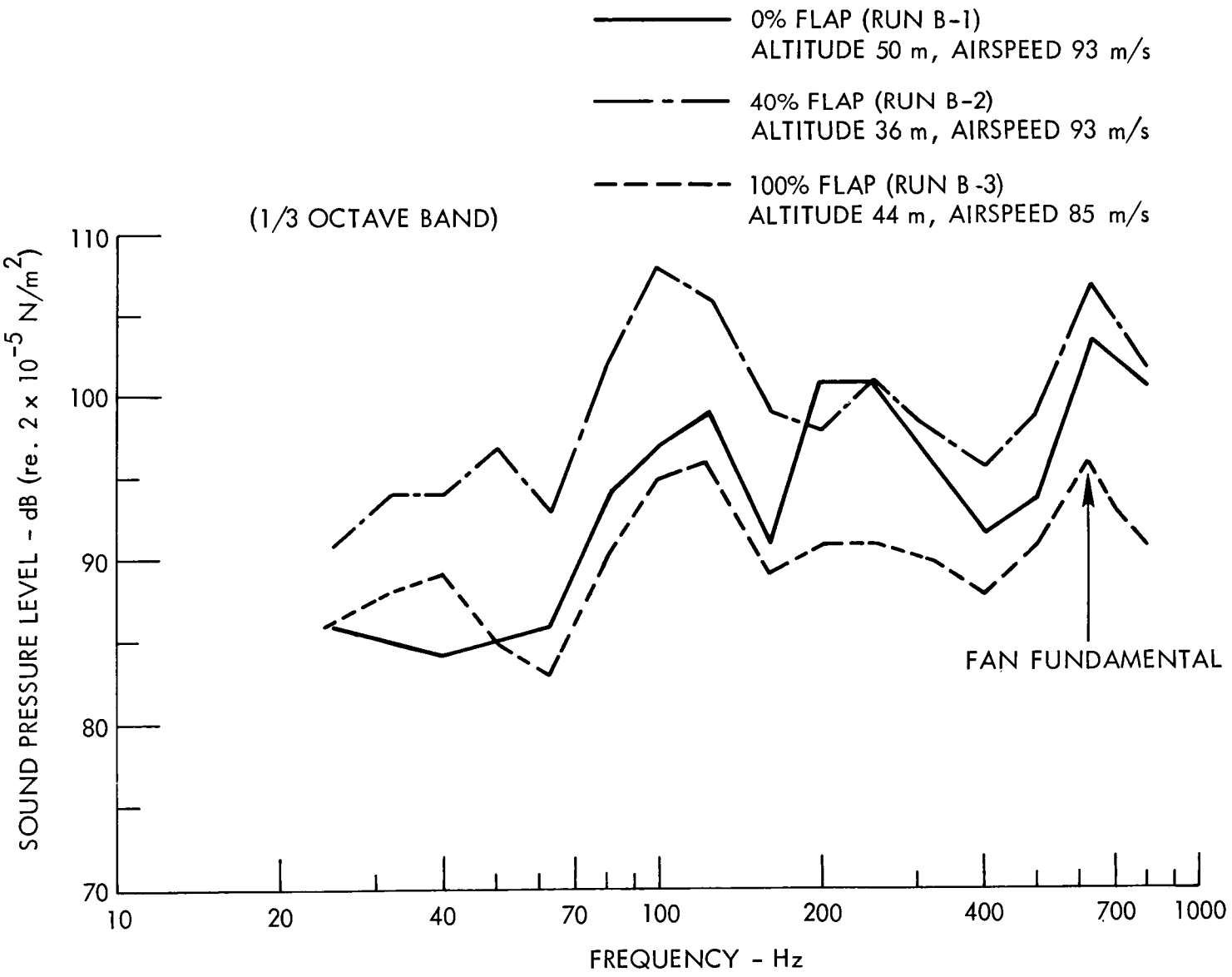

FIGURE 19 NOISE SPECTRA FOR VARIATION OF FLAPS, RETRACTED LANDING GEAR

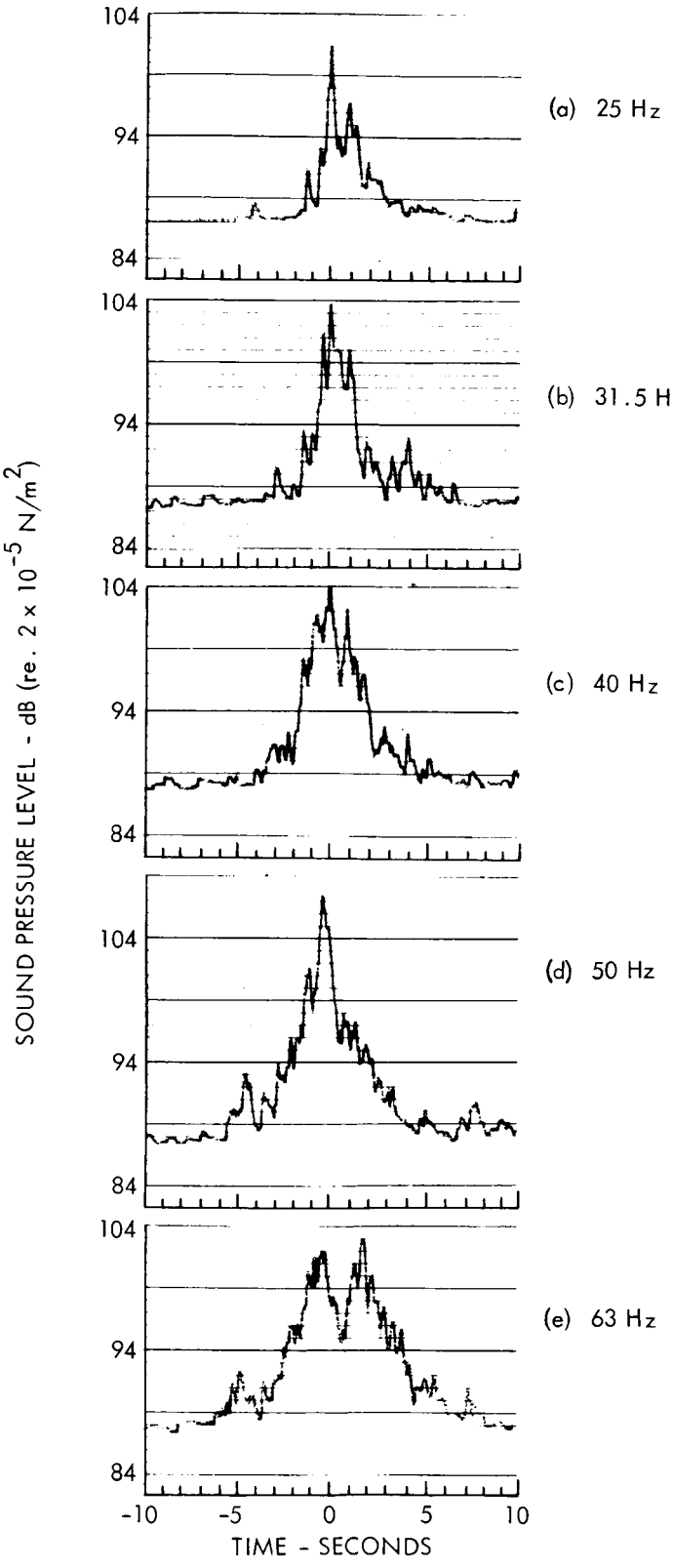

FIGURE 20 AERODYNAMIC NOISE FLYOVER TIME HISTORY (RUN B-2) (1/3 OCTAVE BAND)

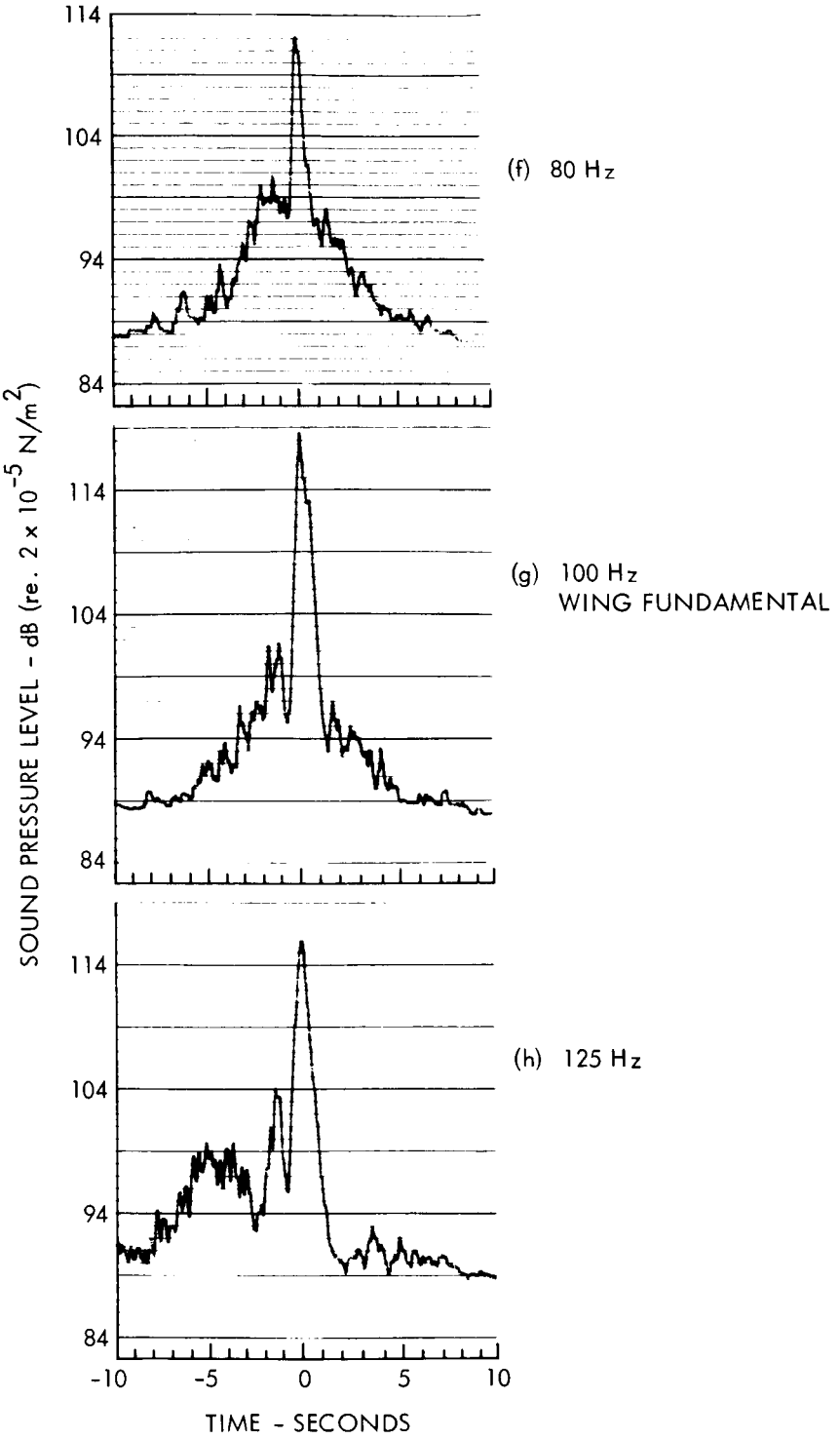

FIGURE 20 AERODYNAMIC NOISE FLYOVER TIME HISTORY (CONTINUED) (RUN B-2) (1/3 OCTAVE BAND)

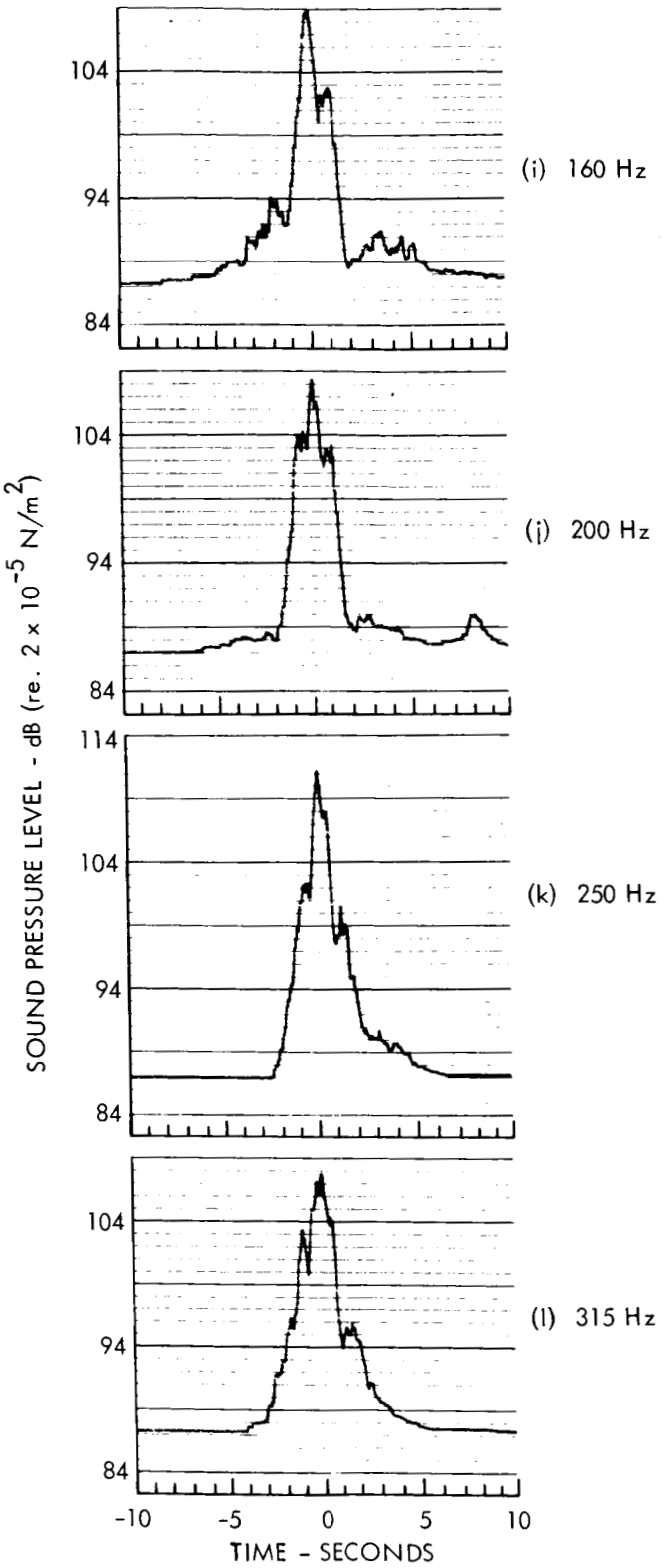

FIGURE 20 AERODYNAMIC NOISE FLYOVER TIME HISTORY (CONTINUED) (RUN B-2) (1/3 OCTAVE BAND)

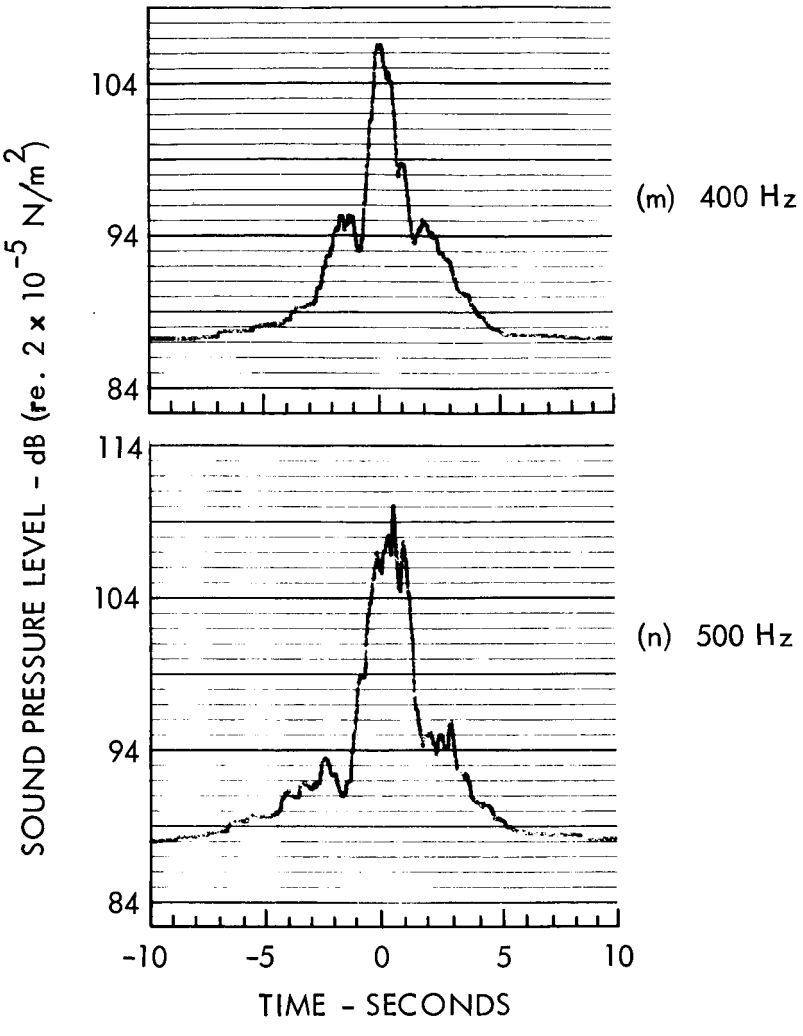

FIGURE 20 AERODYNAMIC NOISE FLYOVER TIME HISTORY (CONTINUED)
(RUN B-2) (1/3 OCTAVE BAND)

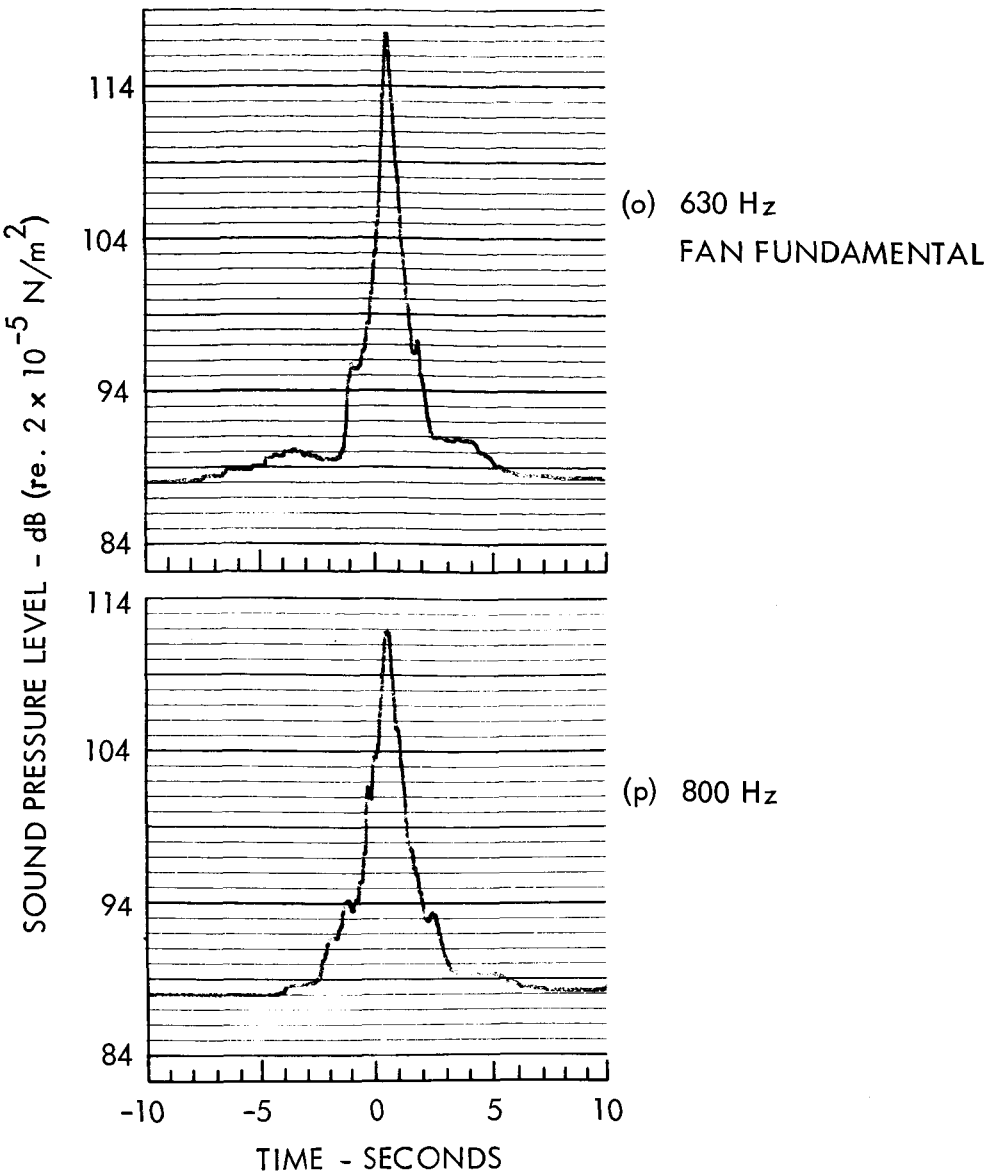

FIGURE 20 AERODYNAMIC NOISE FLYOVER TIME HISTORY (CONTINUED)
(RUN B-2) (1/3 OCTAVE BAND)

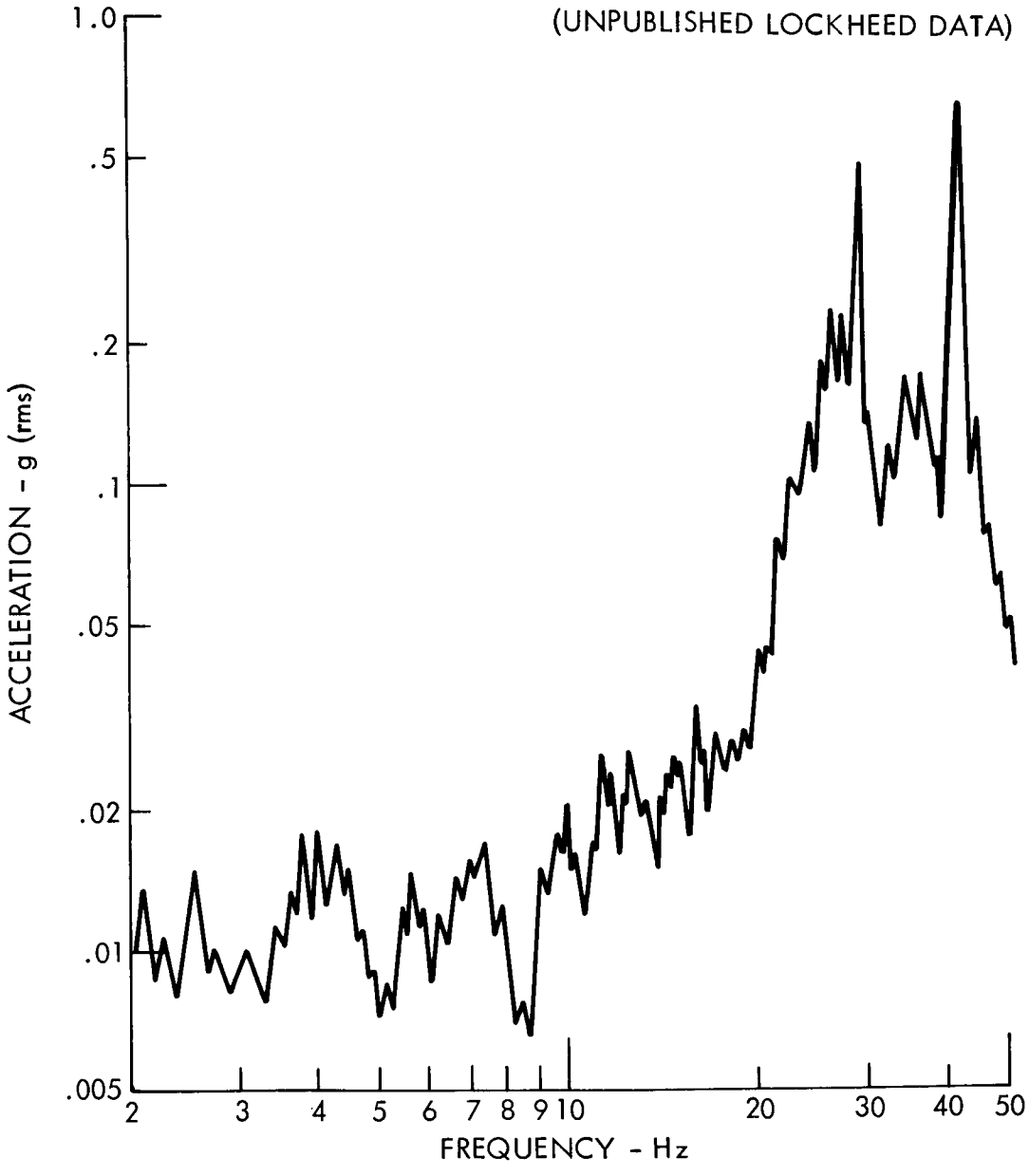

FIGURE 21 WHEEL WELL DOOR VIBRATION

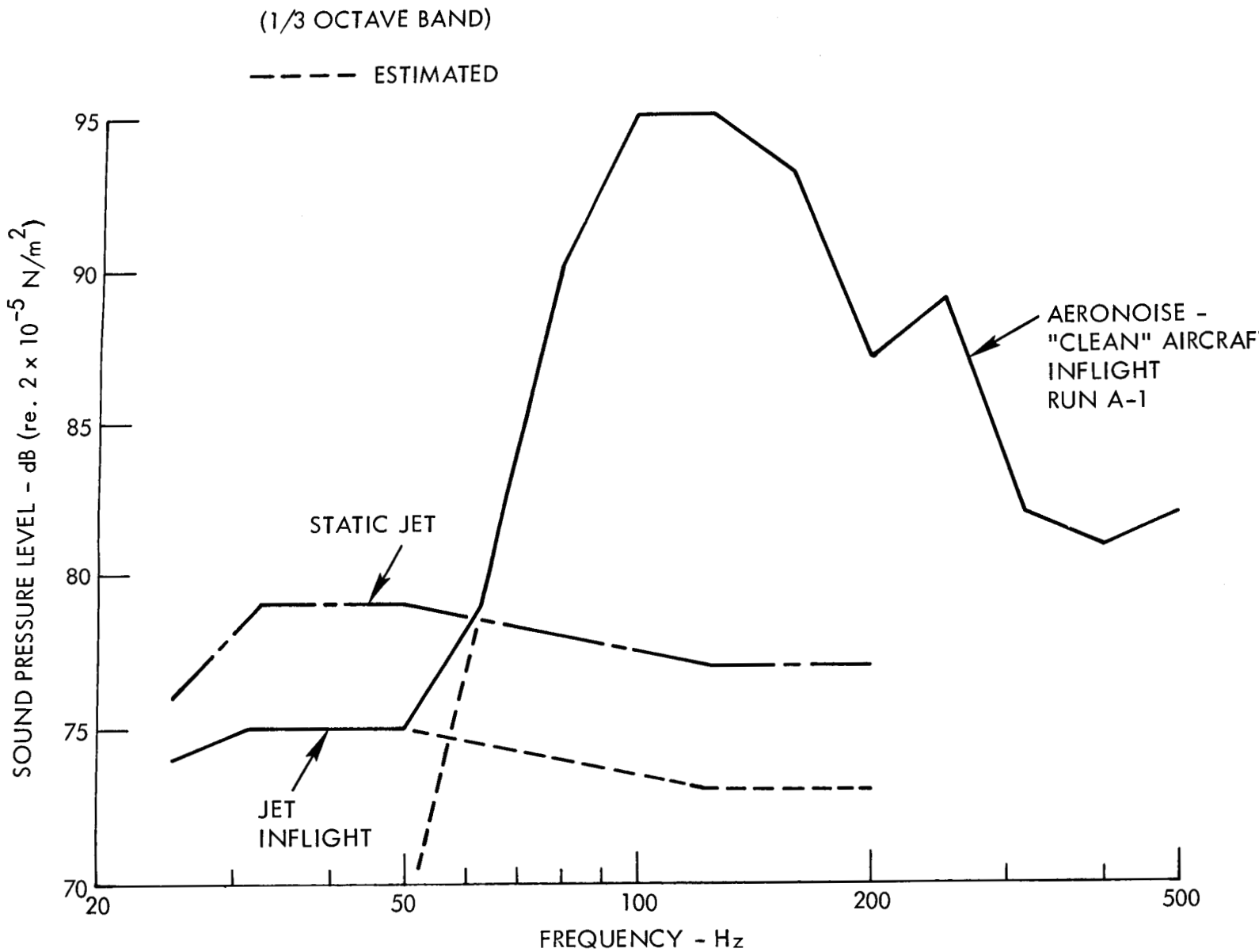

FIGURE 22 INFLIGHT EFFECT ON JET NOISE

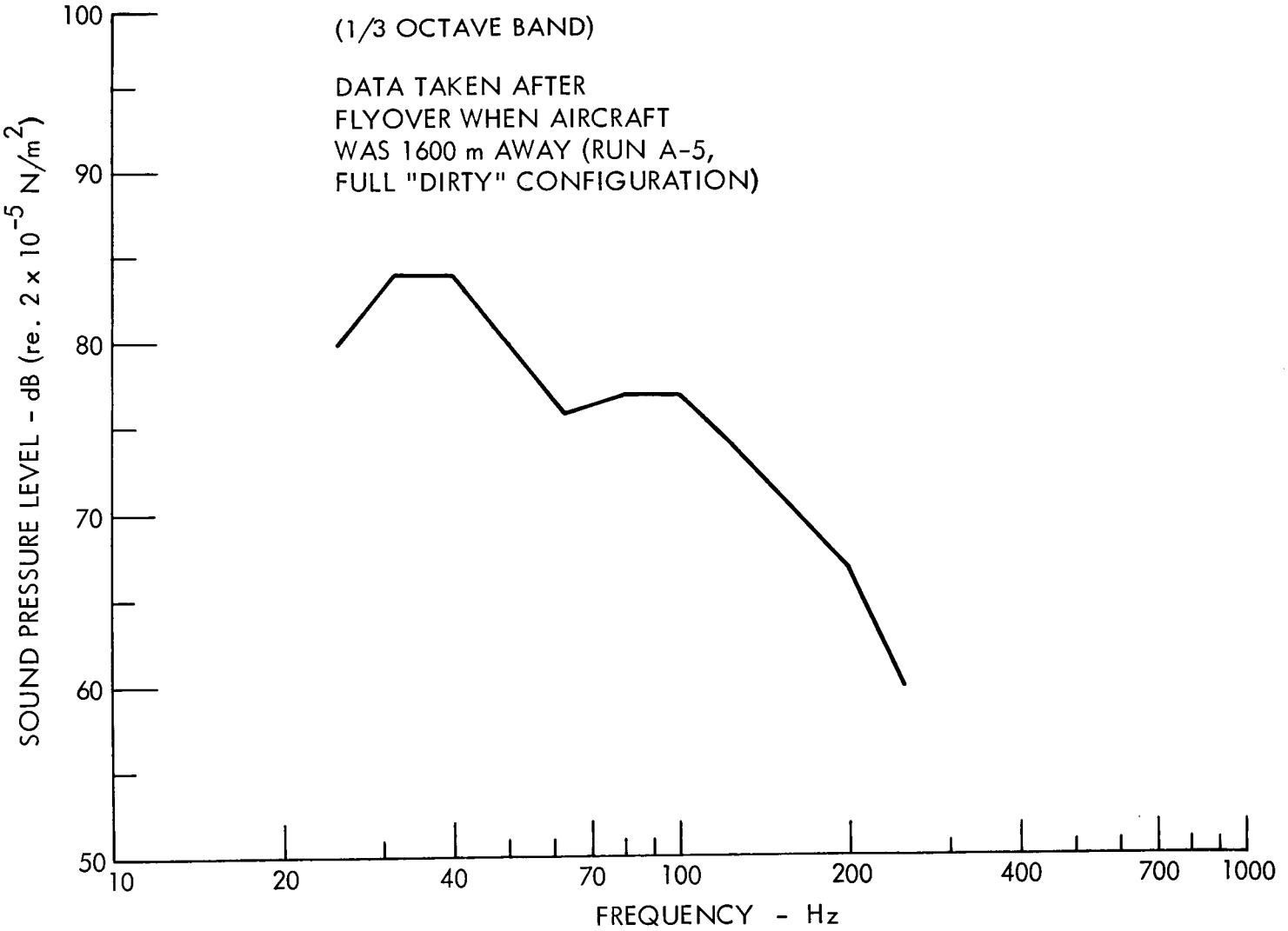

FIGURE 23 GALAXY TRAILING VORTEX NOISE

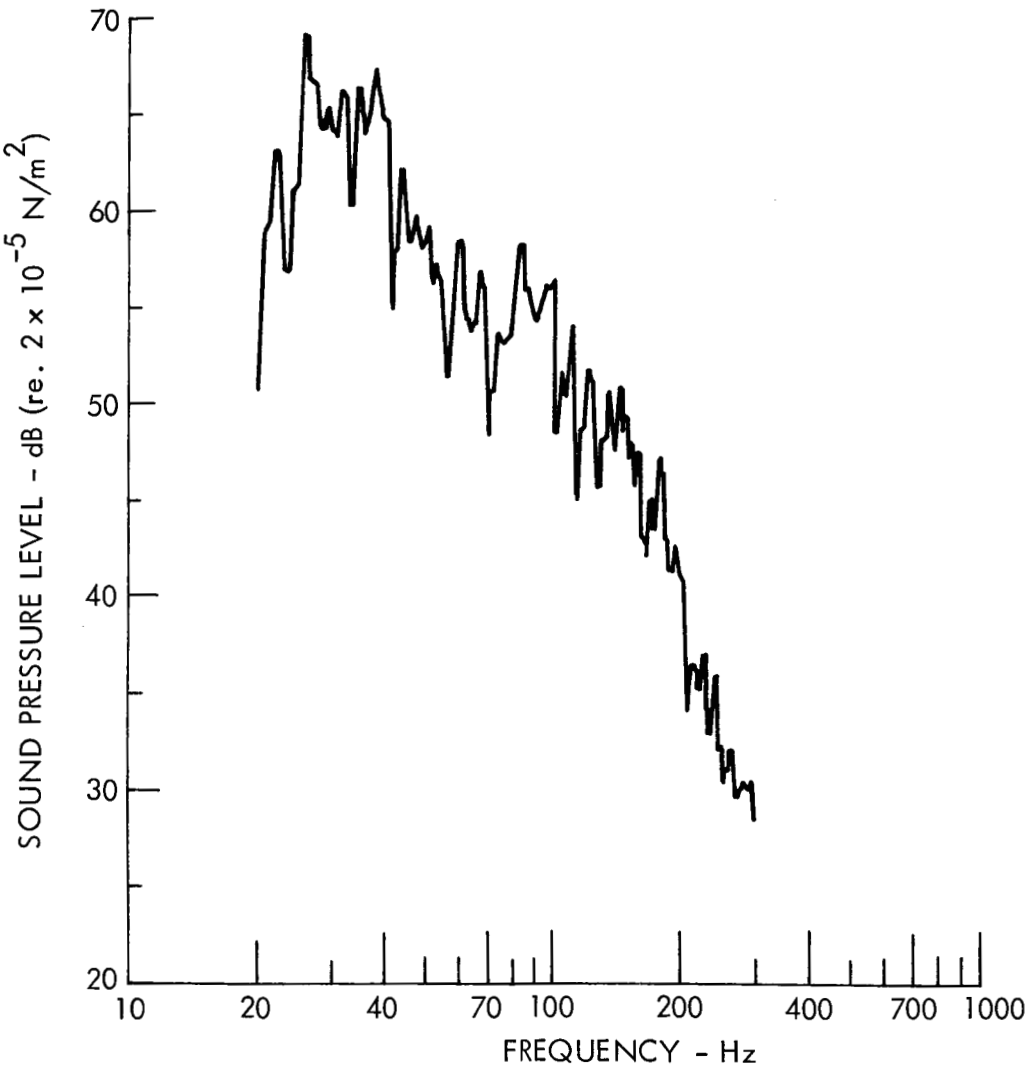

FIGURE 24 NARROW BAND SPECTRUM - TRAILING VORTEX NOISE

APPENDIX

Original Noise Prediction Procedure

Empirical aero noise prediction procedures, based on test results of small aircraft and gliders, were developed under a Lockheed-California Company/Navy program. These procedures predict the overall level and spectrum shape (as discussed in Ref. 2). The maximum overall sound pressure level ($OASPL_{Max}$) is calculated by equation 1.

$$OASPL_{(max)} = 10 \log_{10} \left(\frac{VELOCITY^4}{DISTANCE^2} \cdot \frac{WEIGHT}{CL} \cdot \frac{CHORD}{SPAN} \cdot \frac{PO}{TEMP^2}\right) + CONST \quad (1)$$

where CONST = 27.5 for "clean" configuration aircraft and the other variables as defined under input data on the next page.

The spectrum shape is determined by first calculating the spectrum frequency (f_{max}) at which maximum noise occurs by equation 2.

$$f_{(max)} = \frac{1.85 \times VELOCITY}{T} \quad (2)$$

After $f_{(max)}$ has been determined, a ratio ($TR_i = f_i/f_{max}$) is determined for each one-third-octave-band center frequency (f_i). The differences (ΔSPL_i) between $OASPL_{max}$ and the one-third-octave-band levels (SPL_i) are determined from a generalized empirical curve by entering the curve with successive values of TR_i. This curve can be plotted from values given in the computer program listing (which follows) by using values of TR (lines 3 and 4) as the abscissa, and corresponding values of DELSPL (lines 5 and 6) as the ordinate.

The noise-prediction procedure, with subjective noise-evaluation additions, was incorporated into a computer program that was developed for a UNIVAC 1106 computer with an EXEC-8 software system and a FORTRAN V compiler. The program, designated AIRNOY, calculates $OASPL_{max}$, PNL, EPNL, and one-third-octave-band spectrum at any specified distance for an observer location directly under the aircraft. Perceived Noise Levels are calculated by the PNLREV subroutine using methods presented in SAE ARP 865-A "Definitions and Procedures for Computing Noise Level of Aircraft Noise." Conversion from PNL to EPNL is accomplished by using the AIA empirical conversion curve prepared for the AIA/DOT Noise Certification meeting, Nov. 4, 1968. The use of this curve is provisional, and it is used only to obtain a "Ball Park" EPNL evaluation.

The program has the capability of iterating either velocity or weight (or both) over any desired range to calculate successive noise values for the new parameters. For each increment M (above the value 1), 1000 pounds are added to the aircraft weight, and for each increment N (above the value 1), 10 knots are added to the velocity.

Required input data to the computer program are as follows:

INPUT DATA

FORMAT (2F10.2, 2I10)

VM WM M N

FORMAT (8F10.2)

DIST WEIGHT CL CHORD SPAN VEL PO TEMP

FORMAT (1F10.2)

T

VM = Velocity multiplier

WM = Weight multiplier

M = Weight cases to be run

N = Velocity cases to be run

DIST = Distance from aircraft to observer - ft

WEIGHT = Weight of aircraft - lbs

CL = Coefficient of lift

CHORD = Avg chord length - ft

SPAN = Wing span - ft

VEL = Aircraft velocity - knots

PO = Atmospheric pressure - millibars

TEMP = Atmospheric temperature - °K

T = Average wing thickness - ft

It should be noted that M and N are integers, and all other input is comprised of floating-point numbers. For standard day, sea level conditions, PO = 1040 millibars and TEMP = 294°K.

Following is a listing of the main computer program, a list of the main program variables, and the PNLREV subroutine. Also, two pages of output are given. The input data are printed on the first page along with the calculated noise. The second page is typical of all additional pages which give noise levels for the incremented weight or velocity values.

AIRNOY PROGRAM LISTING

```
      DIMENSION TR(14),DELSPL(14),F(24),D(9),DIF(9),CR(24),RSPL(24),
     1R(24),SPL(24)
      DATA TR/.0156,.0312,.0625,.125,.25,.5,1.0,2.0,4.0,8.0,16.0,32.0,
     164.0,128.0/
      DATA DELSPL/71.,55.,41.,28.,18.,12.,10.,11.,14.,20.,28.,37.,
     148.,60./
      DATA F/50.,63.,80.,100.,125.,160.,200.,250.,315.,400.,500.,
     1630.,800.,1000.,1250.,1600.,2000.,2500.,3150.,4000.,5000.,
     16300.,8000.,10000./
      DATA D/200.,400.,600.,800.,1000.,1200.,1400.,1600.,1800./
      DATA DIF/-5.0,-3.7,-2.2,-1.3,-.4,.3,1.0,1.5,2.2/
      READ(5,501) VM,WM,M,N
      READ(5,502) DIST,WEIGHT,CL,CHORD,SPAN,VEL,PO,TEMP
      READ(5,503) T
C
C     VM            VM TIMES 10 KNOTS = VELOCITY INCREMENT TO BE ADDED
C                   TO INPUT VELOCITY N TIMES
C     WM            WM TIMES 1000 LBS = WEIGHT INCREMENT TO BE ADDED
C                   TO INPUT WEIGHT M TIMES
C     M             NUMBER OF AIRPLANE WEIGHT CASES TO BE RUN
C     N             NUMBER OF AIRPLANE VELOCITY CASES TO BE RUN
C     DIST          FLYOVER ALTITUDE = FT (SOURCE TO OBSERVER DISTANCE)
C     WEIGHT        AIRCRAFT WEIGHT = LBS
C     CL            LIFT COEFFICIENT
C     CHORD         AVERAGE WING CHORD = FT
C     SPAN          WING SPAN = FT
C     VEL           AIRPLANE VELOCITY = KNOTS
C     PO            AMBIENT STATIC PRESSURE = MILLIBARS
C     TEMP          AMBIENT STATIC TEMPERATURE = DEG KELVIN
C     T             AVERAGE MAXIMUM WING THICKNESS = FT
C
  501 FORMAT(2F10.2,2I10)
  503 FORMAT(1F10.2)
  502 FORMAT(8F10.2)
      IF (M) 10,10,11
   11 DO 12 J=1,M
      VEL1=VEL
      DO 13 I=1,N
      EREQM=(1.85*VEL1)/T
      OASPLM=10.0*ALOG10(VEL1**4/DIST**2*WEIGHT/CL*CHORD/SPAN*PO/TEMP
     1**2)+27.5
      DO 20 I=1,24
      DO 19 J=1,14
      CR(I)=F(I)/EREQM
      IF (TR(J)-CR(I)) 19,30,40
   19 CONTINUE
      GO TO 20
   30 RSPL(I)=DELSPL(J)
      GO TO 17
   40 R(I)=(CR(I)-TR(J-1))/(TR(J)-TR(J-1))
      RSPL(I)=DELSPL(J-1)+(R(I)*(DELSPL(J)-DELSPL(J-1)))
   17 SPL(I)=OASPLM-RSPL(I)
```

```
      20 CONTINUE
         PNL=0.0
         CALL PNLREV(SPL,SPH,2)
         DO 84 K=1,9
         IF(D(K)-DIST) 84,85,86
      84 CONTINUE
         GO TO 10
      85 DTE=DTE(K)
         GO TO 83
      86 RATIO=(DIST-D(K-1))/(D(K)-D(K-1))
         DTE=DTE(K-1)+(RATIO*(DTE(K)-DTE(K-1)))
      83 EPNL=SPH+DTE-(10*ALOG10(VEL1/140.0))
         IF(I.EQ.1.AND.J.EQ.1) WRITE(6,601) TEMP, PO,CL,CHORD,T,SPAN,DIST,
        1 WEIGHT,VEL1,OASPLM,EPEQM
         IF(I.NE.1.OR.J.NE.1) WRITE(6,607) WEIGHT,VEL1,OASPLM,EPEQM
         WRITE(6,602) (F(I),SPL(I),I=1,24)
         WRITE(6,604) PNL
         WRITE(6,605) EPNL
     601 FORMAT(1H1,/,2 X,'AIRCRAFT AERODYNAMIC NOISE',//,13X,
        1 'ATMOSPHERIC TEMP.',6X,'=   ',F6.1,' DEG.K',/,13X,
        2 'ATMOSPHERIC PRESSURE   =   ',F6.1,' MIL IBARS',/,13X,
        3 'COEFFICIENT OF LIFT    =    ',F5.2,/,13X,
        4 'AVERAGE CHORD LENGTH   =     ',F5.1,' FEET',/,13X,
        5 'AVERAGE WING THICKNESS =     ',F5.2,' FEET',/,13X,
        6 'WING SPAN              =     ',F5.1,' FEET',/,13X,
        7 'DISTANCE TO OBSERVER   =   ',F6.1,' FEET',/,13X,
        8 'AIRCRAFT WEIGHT        = ',F8.1,' POUNDS',/,13X,
        9 'AIRCRAFT VELOCITY      =   ',F6.1,' KNOTS',/,13X,
        1 'CALCULATED OASPL       =   ',F5.1,' DB',/,13X,
        2 'FREQUENCY OF MAX. SPL  = ',F7.1,' HZ')
     602 FORMAT(//,23X,'FREQUENCY',8X,'SPECTRUM',/,25X,'(HZ)',13X,'(DB)',
        1//,(24X,F7.1,11X,F5.1))
     603 FORMAT(//,25X,'OASPLM',12X,F5.1)
     604 FORMAT(/,26X,'PNL',13X,F5.1)
     605 FORMAT(/,25X,'EPNL',13X,F5.1)
     606 FORMAT(1H1)
     607 FORMAT(1H1,//,13X,'AIRCRAFT WEIGHT        = ',F8.1,
        1 ' POUNDS',/,13X,'AIRCRAFT VELOCITY      =   ',F6.1,' KNOTS',//,
        213X,'CALCULATED OASPL       =   ',F5.1,' DB',/,13X,
        3 'FREQUENCY OF MAX. SPL  = ',F7.1,' HZ')
         DO 92 II=1,24
      92 SPL(II)=0.0
      13 VEL1=VEL1+10.0*KNM
      12 WEIGHT=WEIGHT+1000.0*KNM
         WRITE(6,606)
      10 STOP
         END
```

AIRNOY PROGRAM VARIABLES

CHORD	=	Average wing chord length
CL	=	Coefficient of lift
CR	=	Ratio of frequency to maximum spectrum frequency
D	=	Tabulated distance from aircraft
DELSPL	=	Difference between OASPL and spectrum
DIF	=	Correction for PNL to EPNL (Tabulated)
DIFF	=	Difference between PNL and EPNL
DIST	=	Distance from aircraft to observer
EPNL	=	Effective perceived noise level
F	=	1/3 Octave band frequency
FREQM	=	Spectrum peak frequency
I	=	Do loop counter
II	=	Do loop counter
J	=	Do loop counter
JJ	=	Do loop counter
KK	=	Do loop counter
LL	=	Do loop counter
M	=	Number of weight cases to be run
N	=	Number of velocity cases to be run
OASPLM	=	Overall sound pressure level at observer
PN	=	Perceived noise level at observer
PO	=	Atmospheric pressure
R	=	Interpolation ratio (frequency)
RATIO	=	Interpolation ratio (distance)
RSPL	=	Difference between OASPL and spectrum (Interpolated)
SPAN	=	Wing span
SPL	=	Sound pressure level at observer location
T	=	Wing thickness

TEMP	=	atmospheric temperature
TR	=	Ratio of F/FREQM (tabulated)
VEL	=	Initial velocity of aircraft
VEL 1	=	Aircraft velocity (incremented)
VM	=	Factor to increment velocity
WEIGHT	=	Weight of aircraft
WM	=	Factor to increment weight

PNLREV SUBROUTINE LISTING

```
      SUBROUTINE PNLREV(SPL,PN,NOCT)
      REAL SPL(24),L(5,24),M(4,24),LL(5,8),MM(4,8)
      DATA ((L(I,J),J=1,24),I=1,5)/
     +49.0,44.0,39.0,34.0,30.0,27.0,24.0,21.0,18.0,16.0,16.0,16.0
     1,16.0,16.0,15.0,12.0,9.0,5.0,4.0,5.0,6.0,10.0,17.0,21.0,
     255.0,51.0,46.0,42.0,39.0,36.0,33.0,30.0,27.0,25.0,25.0,25.0,
     325.0,25.0,23.0,21.0,18.0,15.0,14.0,14.0,15.0,17.0,23.0,29.0,
     464.0,60.0,56.0,53.0,51.0,48.0,46.0,44.0,42.0,40.0,40.0,40.0,
     540.0,40.0,38.0,34.0,32.0,30.0,29.0,29.0,30.0,31.0,37.0,41.0,
     691.01,85.88,87.32,79.85,79.76,75.96,73.96,74.91,94.63,100.,100.,
     7100.,100.,100.,100.,100.,100.,100.,100.,100.,100.,100.,44.29,50.72
     8,52.0,51.0,49.0,47.0,46.0,45.0,43.0,42.0,41.0,40.0,40.0,40.0,
     940.0,40.0,38.0,34.0,32.0,30.0,29.0,29.0,30.0,31.0,34.0,37.0/
      DATA((M(I,J),J=1,24),I=1,4)/
     +.07952,.06816,.06816,.05964,10*.053013,.059640,.053013,
     1.053013,.047712,.047712,.053013,.053013,.06816,.07952,.05964,
     2.058098,.058098,.052288,.047534,.043573,.043573,.040221,.037349,
     37*.034859,.040221,.037349,4*.034859,.037349,.037349,.043573,
     4.043478,.040570,.036831,.036831,.035336,.033333,.033333,.032051,
     5.030675,6*.030103,7*.02996,.042285,.042285,15*.030103,9*.02996/
      DATA((LL(I,J),J=1,8),I=1,5)/
     144.0,30.0,21.0,16.0,16.0,9.0,5.0,17.0,
     251.0,39.0,30.0,25.0,25.0,18.0,14.0,23.0,
     360.0,51.0,44.0,40.0,40.0,32.0,29.0,37.0,
     485.88,79.76,74.91,100.,100.,100.,100.,44.29,
     551.0,46.0,42.0,40.0,40.0,32.0,29.0,34.0/
      DATA((MM(I,J),J=1,8),I=1,4)/
     1.068160,6*.053013,.079520,
     2.058098,.043573,.037349,2*.034859,.037349,.034859,.037349,
     3.040570,.035336,.032051,2*.030103,2*.029960,.042285,
     45*.030103,3*.029960/
      IF(NOCT.EQ.2) GO TO 17
C     NOCT=1 OCTAVE BAND INPUT
C     NOCT=2 ONE-THIRD OCTAVE BAND INPUT
      SUM1=0.0
      SUM2=0.0
      DO 26 I=1,8
      IF(SPL(I).GE.LL(1,I)) GO TO 20
      ANOY=0.0
      GO TO 21
   20 IF(SPL(I).GE.LL(2,I)) GO TO 22
      ANOY=.1*10.0**(MM(1,I)*(SPL(I)-LL(1,I)))
      GO TO 21
   22 IF(SPL(I).GE.LL(3,I)) GO TO 23
      ANOY=10.0**(MM(2,I)*(SPL(I)-LL(3,I)))
      GO TO 21
   23 IF(SPL(I).GE.LL(4,I)) GO TO 24
      ANOY=10.0**(MM(3,I)*(SPL(I)-LL(3,I)))
      GO TO 21
   24 IF(SPL(I).GT.150.0) GO TO 25
      ANOY=10.0**(MM(4,I)*(SPL(I)-LL(5,I)))
      GO TO 21
   25 WRITE(6,602)
  602 FORMAT(///,10X,'SPL EXCEEDS 150 DB',///)
      GO TO 101
   21 IF(ANOY.LE.SUM2) GO TO 26
```

```
57              SUM2=ANOY
58           26 SUM1=SUM1+ANOY
59              IF(SUM1.LT.0.01) GO TO 30
60              IF(SUM2.LT.0.01) GO TO 30
61              IF(SUM2.GT.SUM1) GO TO 30
62              PN=40.0+33.22*ALOG10(SUM2+.3*(SUM1-SUM2))
63          101 RETURN
64           17 SUM1=0.0
65              SUM2=0.0
66              DO 16 I=1,24
67              IF(SPL(I).GE.L(1,I)) GO TO 10
68              ANOY=0.0
69              GO TO 11
70           10 IF(SPL(I).GE.L(2,I)) GO TO 12
71              ANOY=.1*10.0**(M(1,I)*(SPL(I)-L(1,I)))
72              GO TO 11
73           12 IF(SPL(I).GE.L(3,I)) GO TO 13
74              ANOY=10.0**(M(2,I)*(SPL(I)-L(3,I)))
75              GO TO 11
76           13 IF(SPL(I).GE.L(4,I)) GO TO 14
77              ANOY=10.0**(M(3,I)*(SPL(I)-L(3,I)))
78              GO TO 11
79           14 IF(SPL(I).GT.150.) GO TO 15
80              ANOY=10.0**(M(4,I)*(SPL(I)-L(5,I)))
81              GO TO 11
82           15 WRITE(6,601)
83          601 FORMAT(///,10X,'SPL EXCEEDS 150 DB',///)
84              GO TO 100
85           11 IF(ANOY.LE.SUM2) GO TO 16
86              SUM2=ANOY
87           16 SUM1=SUM1+ANOY
88              IF(SUM1.LT.0.01) GO TO 30
89              IF(SUM2.LT.0.01) GO TO 30
90              IF(SUM2.GT.SUM1) GO TO 30
91              PN=40.0+33.22*ALOG10(SUM2+.15*(SUM1-SUM2))
92              GO TO 100
93           30 PN=0.0
94          100 RETURN
95              END
```

AIRCRAFT AERODYNAMIC NOISE

ATMOSPHERIC TEMP.	= 294.0	DEG.K
ATMOSPHERIC PRESSURE	= 1040.0	MILLIBARS
COEFFICIENT OF LIFT	= 1.03	
AVERAGE CHORD LENGTH	= 28.3	FEET
AVERAGE WING THICKNESS	= 2.81	FEET
WING SPAN	= 219.0	FEET
DISTANCE TO OBSERVER	= 300.0	FEET
AIRCRAFT WEIGHT	= 613000.0	POUNDS
AIRCRAFT VELOCITY	= 168.0	KNOTS

CALCULATED OASPL	= 96.6	DB
FREQUENCY OF MAX. SPL	= 110.6	HZ

FREQUENCY (HZ)	SPECTRUM (DB)
50.0	83.5
63.0	84.9
80.0	85.5
100.0	86.2
125.0	86.5
160.0	86.2
200.0	85.8
250.0	85.2
315.0	84.4
400.0	83.2
500.0	81.9
630.0	80.1
800.0	77.8
1000.0	75.6
1250.0	73.3
1600.0	70.2
2000.0	67.5
2500.0	64.9
3150.0	61.6
4000.0	58.2
5000.0	55.1
6300.0	51.1
8000.0	47.1
10000.0	43.7
PNL	99.4
EPNL	94.2

STANDARD PRINTOUT

AIRCRAFT WEIGHT = 614000.0 POUNDS
AIRCRAFT VELOCITY = 168.0 KNOTS

CALCULATED OASPL = 96.[illegible] DB
FREQUENCY OF MAX. SPL = 110.6 HZ

FREQUENCY (HZ)	SPECTRUM (DB)
50.0	83.5
63.0	84.9
81.0	85.[illegible]
10[illegible].0	86.3
125.0	86.5
160.0	86.2
200.0	85.[illegible]
250.0	85.2
315.0	84.[illegible]
400.0	83.2
500.0	81.9
630.0	80.1
800.0	77.8
1000.0	75.6
1250.0	73.[illegible]
1600.0	71.2
2000.0	67.5
2500.0	64.9
3150.0	61.[illegible]
4000.0	58.2
5000.0	55.1
6300.0	51.1
8000.0	47.1
10000.0	43.7
PNL	99.4
EPNL	94.2

OPTIONAL PRINTOUT

REFERENCES

1. Smith, D. L., et al.: Measurements of the Radiated Noise from Sailplanes. FDL TM-70-3-FDDA, Wright-Patterson AFB, Ohio, 1970.

2. Gibson, J. S.: The Ultimate Noise Barrier - Far Field Radiated Aerodynamic Noise. Inter Noise 72 Proceedings, p. 332, Washington, D.C., 1972.

3. Paterson, R. W., et al.: Vortex Shedding Noise of an Isolated Airfoil. United Aircraft Research Laboratories, Technical Report K810867, 1971.

4. Graham, R. R.: The Silent Flight of Owls. Journal of the Royal Aeronautical Society, Vol. 38, 1934.

5. Bishop, D. E.: Frequency Spectrum and Time Duration Descriptions of Aircraft Fly-over Noise Signals. FAA DS-67-6, 1967.

6. Eldred, K., Roberts, W., and White, R.: Structural Vibrations in Space Vehicles, Section III Aerodynamic Excitation. Northrop Corporation, WADD TR61-62, 1961.

7. Theisen, J. G., Haas, J.: Turbulence Upset and Other Studies on Jet Transports. Journal of Aircraft, Vol. 5, No. 4, 1968.

8. Gibson, J. S.: Non-Engine Aerodynamic Noise: The Limit to Aircraft Noise Reduction. Inter-Noise 73 Proceedings, Copenhagen, 1973.

9. Blumenthal, V. L., et al.: Aircraft Environmental Problems. AIAA Paper 73-5, Washington, D.C., 1973.